Dopamine D_2 and Adenosine A_{2A} Receptors Interaction on Ca^{2+} Current Modulation in a Rodent Model of Parkinsonism

Ernesto Alberto Rendón-Ochoa[1], Montserrat Padilla-Orozco[2],
Vladimir Melesio Calderon[2] , Victor Hugo Avilés-Rosas[2],
Omar Hernández-González[3], Teresa Hernández-Flores[4],
María Belén Perez-Ramirez[2], Marcela Palomero-Rivero[2],
Elvira Galarraga[2] and José Bargas[2]

Abstract

Adenosine A_1 and A_{2A} receptors are expressed in striatal projection neurons (SPNs). A_1 receptors are located in direct (dSPN) and indirect SPNs (iSNP). A_{2A} receptors are only present in iSPNs. Dopamine D_2 receptors are also expressed in iSPNs and interactions between D_2 and A_{2A} receptors have received attention. iSPNs activity increases during parkinsonism (PD) and A_{2A} receptors may be responsible by enhancing Ca^{2+} currents (iCa^{2+}). Therefore, A_{2A} receptors blockade is a therapeutic approach. We asked whether A_{2A} receptors need the interaction with D_2 receptors (D_2R) to exert their actions. By using isolated and identified iSPNs to avoid indirect influences, we show that D_2R action habilitates A_{2A} receptors ($A_{2A}R$) modulation. iCa^{2+} through voltage gated Ca^{2+} channels (Ca_V) was used as a signal to observe this interaction. Voltage-clamp recordings in acutely dissociated iSPNs, current-clamp recordings in slices and calcium imaging in transgenic A_{2A}-Cre mice, showed that D_2R reduction in iCa^{2+} endows $A_{2A}R$ to restore iCa^{2+} on iSPNs showing an antagonistic interaction between D_2 and A_{2A} receptors. A_{2A} receptors were blocked by the antagonist istradefylline, however, this blockade differed in control and dopamine-depleted iSPNs: istradefylline reduced D_2R modulation in parkinsonian animals as compared to controls. Calcium imaging recordings show that istradefylline occludes D_2R actions in the parkinsonian circuitry and this effect depends on the order of drugs application. Thus, while D_2 activation enables A_{2A} receptors action, blockade of $A_{2A}R$ induces a reduction in the action of D_2 agonists, confirming a complex interaction.

Summary Statement

A_{2A} receptor required previous D_2 receptor activation to modulate Ca^{2+} currents. Istradefylline decreases pramipexole modulation on Ca^{2+} currents. Istradefylline reduces A_{2A} + neurons activity in striatial microcircuit, but pramipexole failed to further reduce neuronal activity.

Keywords

[1]Laboratorio de Psicofarmacología, Unidad de Investigación Interdisciplinaria y de Ciencias de la Salud y Educación, Facultad de Estudios Superiores Iztacala, Universidad Nacional Autónoma de México, Tlalnepantla, Mexico
[2]División de Neurociencias, Instituto de Fisiología Celular, Universidad Nacional Autónoma de México, Ciudad de Mexico, Mexico
[3]Facultad de Medicina, Departamento dé Fisiología, Universidad Nacional Autónoma de México, Circuito Exterior s/n Ciudad Universitaria, Ciudad de Mexico, Mexico
[4]Brain Mechanism for behavior Unit, Okinawa Institute of Science and Technology, Okinawa, Japan

Corresponding Author:
José Bargas, División de Neurociencias, Instituto de Fisiología Celular, Universidad Nacional Autónoma de México, 04510 México D.F. México.
Email: jbargas@ifc.unam.mx

Introduction

The main drug for Parkinson's disease treatment is 3-(3,4-dihydroxyphenyl)-L-alanine (L-DOPA) (e.g.: Mercuri & Bernardi, 2005), although its long-term use entails motor complications such as L-DOPA induced dyskinesias and on/off phenomena (Berthet & Bezard, 2009; LeWitt & Fahn, 2016; Reddy et al., 2014). These are more frequent and appear sooner when using higher doses of L-DOPA (Olanow & Schapira, 2013).

Dopaminergic agonists such as pramipexole may retard these phenomena, although their actions do not completely match those of L-DOPA (Lara-Gonzalez et al., 2019; Millan, 2010). Therefore, non-dopaminergic drugs have been proposed as adjuvants to increase L-DOPA useful time and reduce motor complications.

Parkinsonism exhibits an overactivation of indirect striatal projection neurons (iSNP) and the striatal circuit in general (Jáidar et al., 2010, 2019; Kravitz et al., 2010; Zhai et al.,
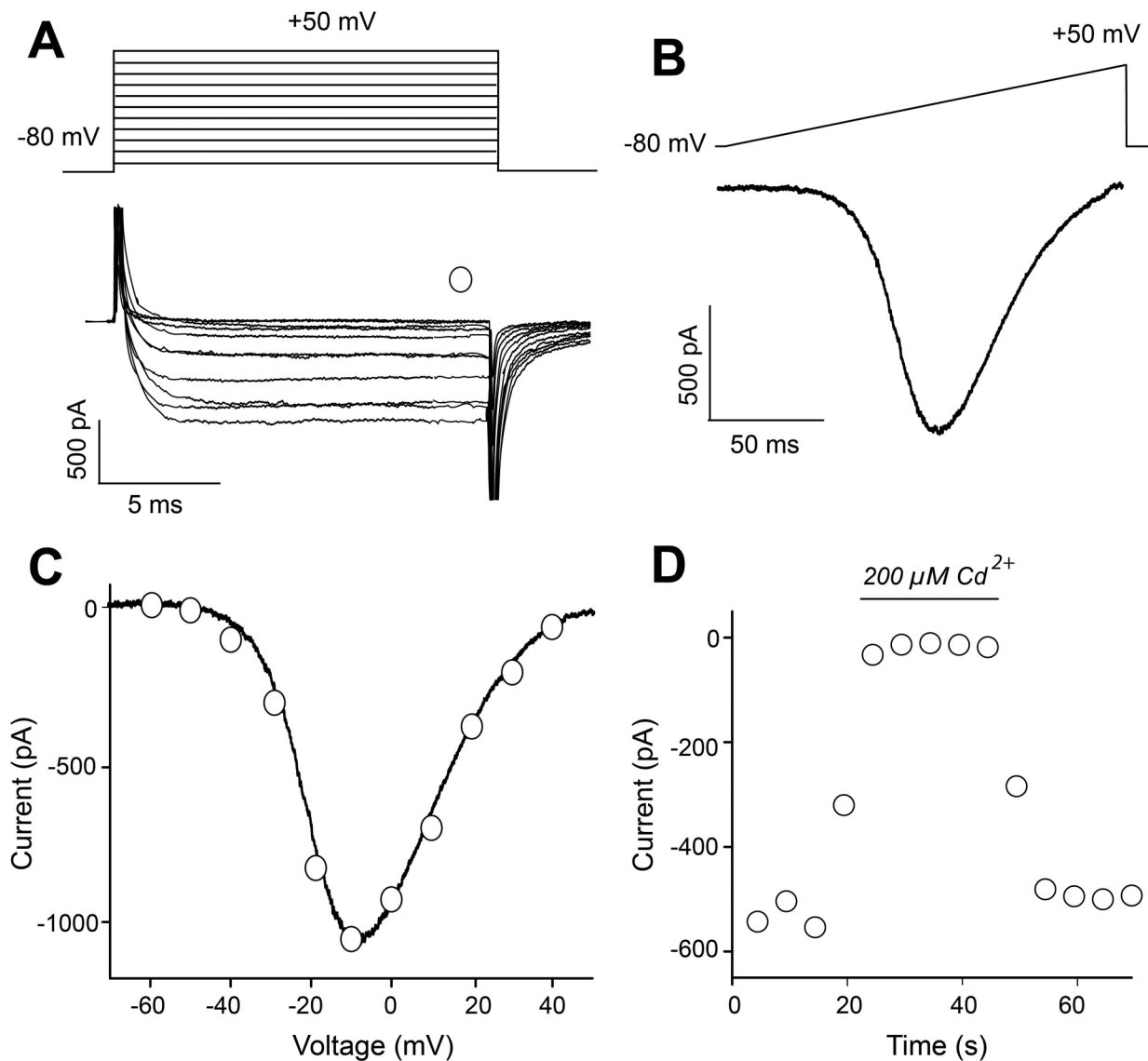
Figure 1. Whole-cell Ca^{2+} currents in acutely dissociated A_{2A} receptor expressing indirect striatal projection neurons (iSPNs). A) Representative inward Ca^{2+} current (bottom) elicited by rectangular voltage commands from -80 to $+50$ mV (top) in 10 mV steps (tail currents are clipped). Empty circles show where Ca^{2+} current amplitude was taken. The cells were in presence of TTX and Ba^{2+} (see Methods), therefore, no Na^+ or K^+ currents were elicited. B) Ca^{2+} currents (bottom) in the same neuron evoked by a ramp voltage command from -80 to $+50$ mV (top) in 0.7 mV/ms (tail currents are not shown). C) Current-voltage relationship (I-V plot) showing superimposed measurements from currents obtained with rectangular voltage commands in A (empty circles) and ramp commands in B (continuous line). Note that current obtained with the ramp command "fits" measurements of currents obtained with rectangular commands, suggesting good voltage control and space clamp. D) Representative time course of Ca^{2+} currents blockade during bath application of 200 μM Cd^{2+} in a different cell.
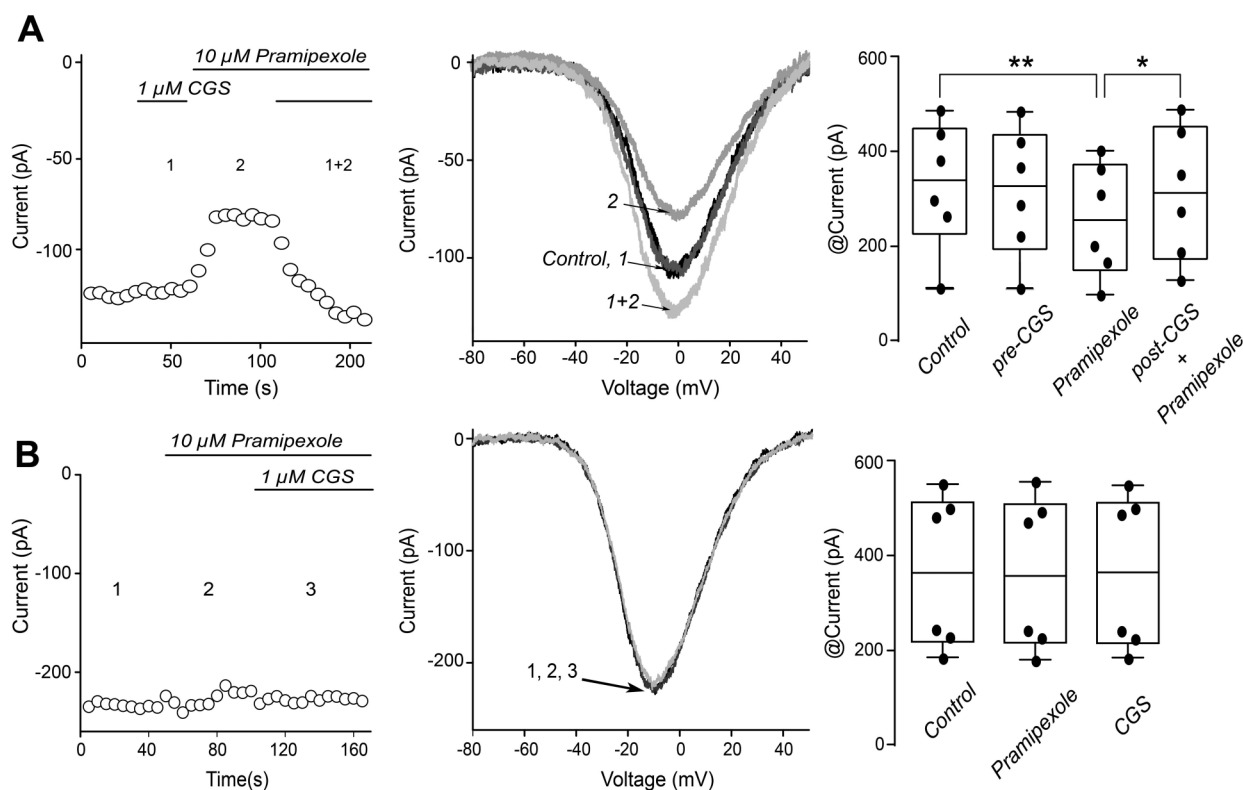
Figure 2. Demonstration of D_2-A_{2A} receptors interaction: application of a selective adenosine A_{2A} receptor agonist only modulates Ca^{2+} current when dopamine D_2 receptors are previously activated. A) Left: time course of drugs actions on Ca^{2+} currents: 1 μM of CGS-21680 (CGS) applied alone has no effect on whole cell Ca2 + currents in isolated indirect SPNs (identified A_{2A} receptor expressing neurons) (1). 10 μM pramipexole, a dopamine $D_{2/3}$ receptor selective agonist, reduces Ca^{2+} currents (2). In the presence of pramipexole, administration of CGS increases Ca^{2+} currents reversing the action of pramipexole (3). Middle: I-V plots taken at different moments during the time course at left. Results suggest that A_{2A} receptors action requires a previous activation of D_2 receptors. Right: box plots summarize these results in a sample of neurons using absolute current amplitudes (n = 6 neurons from different slices and animals; Friedman ANOVA with post hoc Dunnet tests. F(3) = 12.60. Control vs. pramipexole: ** P = .004 and pramipexole vs. pramipexole plus CGS: * P = .04). There were no significant differences between CGS given alone and CGS plus pramipexole. B) Left: representative time course of Ca^{2+} currents amplitude showing that neither application of 10 μM pramipexole alone nor addition of 1 μM CGS have any effects on Ca^{2+} currents in A_{2A} negative neurons (putative direct SPNs). Middle; I-V plots taken from the time course at left. Box plots at right summarize these results with absolute current amplitudes (n = 6 from different slices and n = 3 different animals; Friedman ANOVA test. F(2) = 4. P = .184).

2018). How much of this overactivation is due to D_2-A_{2A} receptors interaction (Ferré & Fuxe 1992; Hillion et al., 2002) is currently debated (Beggiato et al., 2014; Fredholm et al., 2011; Preti et al., 2015). A_{2A} receptors (A_{2A}R) activation activates the Golf/s/cAMP/PKA cascade in iSPNs (Fredholm et al., 2000; Jacobson & Gao, 2006) increasing Ca^{2+} currents (iCa^{2+}) and excitability (Hernandez-Gonzalez, et al., 2014; Hernandez-Lopez et al., 1997) and N-methyl-D-Aspartate (NMDA) plateau potentials (Azdad et al., 2009). iSPNs hyperexcitability is reduced by A_{2A}R antagonists (Armentero et al., 2011; Moreau & Huber, 1999; Muller & Ferré, 2007; Preti et al., 2015; Richardson et al., 1997; Tozzi et al., 2007; Yabuuchi, et al., 2006), effective in improving motor deficits in parkinsonian (PD) patients (Hauser et al., 2011; Mizuno et al., 2010; Müller, 2015; LeWitt 2008; Stacy, 2009), 1-methyl-4-phenyl-l,2,3,6-tetrahydropyridine (MPTP) PD macaques (Ko et al., 2016), dopamine-depleted rats (Bové et al., 2002) and mice (Matsuya et al., 2007).

Hence, one aim of the present study was to observe whether A_{2A}R actions depend on a previous habilitation by D_2R, thus involving D_2-A_{2A} receptors interaction. Indeed, we demonstrate this interaction (Fuxe et al., 2010) by using A_{2A}-Cre mice to identify iSPNs and by recording acutely dissociated neurons to avoid indirect actions. Ca^{2+} current was seen as a signaling effector in the dorsal striatum, in the nucleus accumbens, globus pallidus and cell lines (Azdad et al., 2009; Floran et al., 2005; Salim et al., 2000). Similarly, activation of A_{2A}R requires the previous activation of adenosine A_1 receptors in the dorsal striatum (Hernandez-Gonzalez et al., 2014), and as D_2R, A_1 receptors probably use the PLC cascade to reduce iCa^{2+} (Hernandez-Lopez et al., 2000; Jacobson & Gao, 2006; Preti et al., 2015). Here we demonstrate that previous D_2R reduction of iCa^{2+} is necessary for a A_{2A}R agonist to increase and restore iCa^{2+} on iSPN, thus counteracting D_2R modulation and revealing a functional antagonism between both receptors (Ferré et al., 1991, 2008; Stromberg et al., 2000) on iCa^{2+}
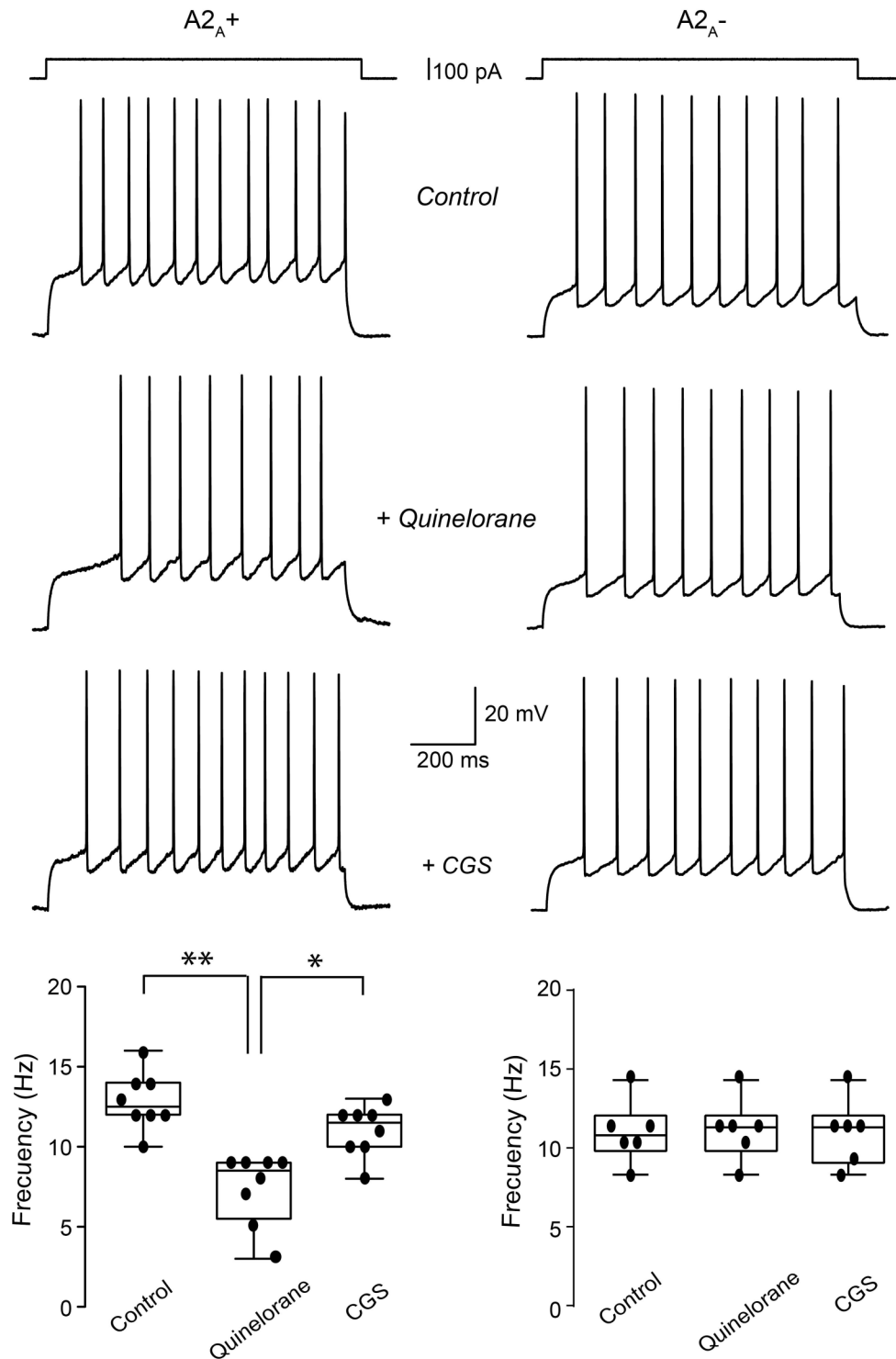
Figure 3. Action of A_{2A} receptors on excitability of indirect SPNs after the previous activation of D_2 receptors. Evoked firing after 100 pA somatic current injections in all cases. Left column: top: control firing, middle: application of 10 μM quinelorane, a D_2 receptors agonist, decreases firing frequency in indirect SPNs ($A_{2A}+$) from 12.8 ± 0.63 to 7.37 ± 0.8 Hz. CGS application, in the continuous presence of quinelorane, restores firing frequency from 7.37 ± 0.8 to 11 ± 0.6 Hz (bottom). Right column: quinelorane failed to significantly decrease frequency in putative direct SPNs ($A_{2A}-$ neurons). Box plots at the left summarizes the results in a sample of indirect SPNs in all three conditions (n = 8 from 8 different slices and from 8 animals, Friedman ANOVA with post hoc Dunnet tests. $F_{(2)} = 13.87$. **$P = .0014$, *$P = .0374$). Box plot at the right summarizes the action of quinerolane and CGS in putative dSPNs, no differences were found (n = 7 from 7 different slices and from 7 animals, Friedman ANOVA with post hoc Dunnet tests. $F_{(2)} = 1$, $P > .999$).
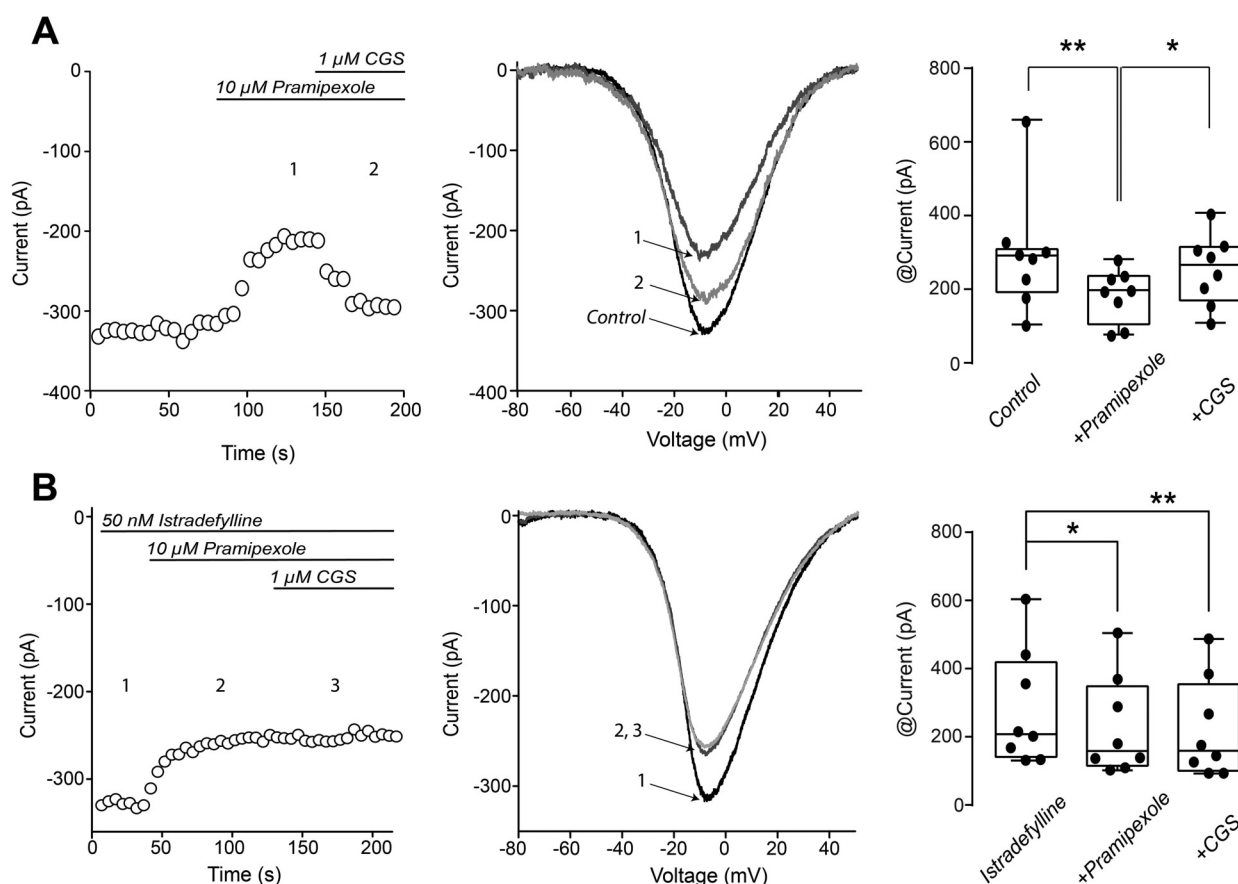
Figure 4. Istradefylline, a selective A_{2A} receptor antagonists, blocks CGS agonist action in the presence of pramipexole in neurons from control neurons (non-dopamine depleted). A) Left: representative time course of Ca^{2+} currents reduction by 10 μM pramipexole application (1). The subsequent action of CGS partially restored Ca^{2+} currents in the continuous presence of pramipexole (2). Middle: I-V plots taken at the indicated stages of the time course at left. Pramipexole decreased Ca^{2+} currents in identified indirect SPNs (A_{2A}+ neurons) by (mean ± S.E.M.) 31.9 ± 6%. The subsequent application of CGS partially restored Ca^{2+} currents in all A_{2A}+ neurons to 255 ± 32 pA (an increase of 22.5 ± 4.72%). Right: box plots summarize results from these samples of neurons (absolute current amplitudes are shown; n = 8 neurons taken from 8 different slices and 8 animals, Friedman ANOVA with post hoc Dunnet tests. F(2) = 12.25. Control vs. pramipexole: **P = .0035 and pramipexole vs. pramipexole plus CGS: *P = .0179). B) Left: similar representative time course in another indirect SPN in the continuous presence of 50 nM istradefylline. Notice that the action of pramipexole is present: Ca^{2+} currents was decreased by 25.7 ± 3% whereas the action of CGS is suppressed by istradefylline, confirming that CGS acted on A_{2A} receptors. Middle: I-V plots taken at indicated stages of the time course at left. Right: box plots summarize these results using absolute current amplitudes (n = 8 neurons taken from 8 different slices and animals; Friedman ANOVA with post hoc Dunnet tests F(2) = 13.00. *P = .0374; **P = .0014).

amplitude and excitability, showing a molecular correlate of behavioral and pharmacological findings (Ferré et al., 2008; Prasad et al., 2021). The selective antagonist istradefylline, blocked the action of A_{2A}R. However, istradefylline blockade differed between control and dopamine-depleted iSPN: A_{2A} receptors blockade reduced the modulation of D_2R on iCa^{2+} of dopamine-depleted iSPNs from parkinsonian animals; perhaps, a physiological correlate of D_2R affinity decrease by A_{2A}R ligands (Bonaventura et al., 2015; Preti et al., 2015).

In addition, we show the reduction in hyperexcitability by A_{2A}R blockade on dozens of simultaneously active iSPN from parkinsonian 6-OHDA mice. In particular, we found differences in A_{2A}R blockade when antagonists of these receptors are administered after or before the actions of D_2R agonists. In these conditions, with iSPNs interconnected within their network receiving multiple influences, A_{2A}R antagonism virtually occludes D_2R actions when applied before the dopamine-agonist.

Materials and Methods

Research Subjects

Protocols were designed and performed in accordance with the international norms for the ethical use of experimental animals established in the National Institutes of Health Guide for Care and Use of Laboratory Animals Eighth Edition (NIH, 2010)*, including minimizing the number of animals to achieve statistical significance and the avoidance of animal suffering. The mouse strain used for this work, Tg(Adora2a-cre)KG139Gsat/ Mmucd, RRID:MMRRC_031168-UCD, was obtained from
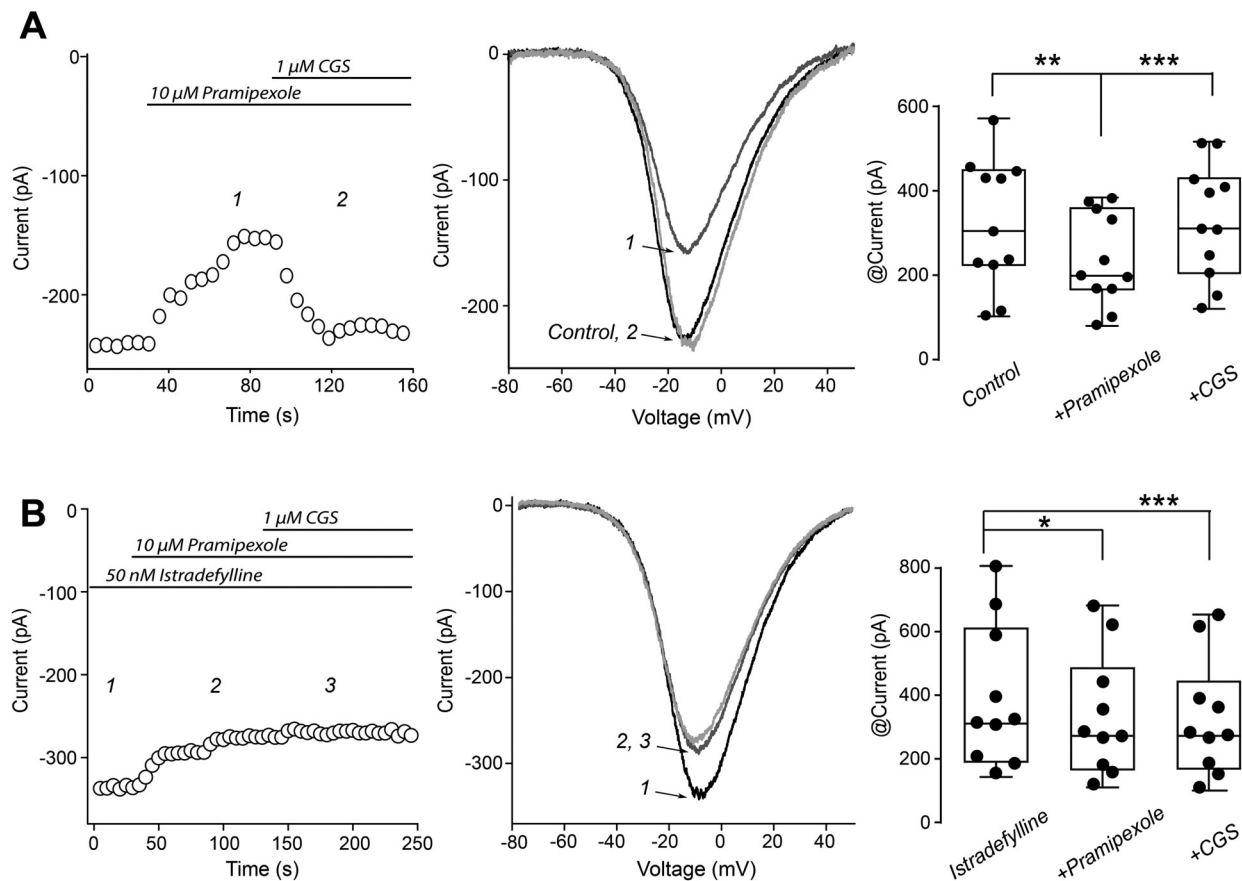
**Figure 5.** Istradefylline, a selective A_{2A} receptor antagonist, blocks CGS action in the presence of pramipexole in dopamine-depleted indirect SPNs. A) Left: representative time course of Ca^{2+} currents reduction by 10 μM pramipexole application. Reduction was $23.7 \pm 3.46\%$. The subsequent action of CGS restored Ca^{2+} currents in the continuous presence of pramipexole in identified indirect SPNs ($A_{2A}+$ neurons) to $38 \pm 5.26\%$. Middle: I-V plots taken from the time course at left as indicated by numbers. Right: box plots summarize results from these samples of neurons using absolute Ca^{2+} currents amplitudes (n = 11 neurons taken from 10 different animals; Friedman ANOVA test with post hoc Dunnet tests F(2) = 16.55. Control vs. pramipexole: **$P = .002$; pramipexole vs. pramipexole plus CGS: ***$P = .0009$), showing restoration of Ca^{2+} currents by CGS in dopamine-depleted neurons. B) Left: similar experiment as in (A) but in the continuous presence of the A_{2A} receptor antagonist, istradefylline: pramipexole keeps having a reducing effect of $14.9 \pm 2.2\%$ on Ca^{2+} currents but the counteracting action of CGS was blocked. Middle: I-V plots taken from the time course at left as indicated. Box plot summarize the results from these samples of neurons using absolute current amplitudes (n = 10 neurons taken from 9 different animals; Friedman ANOVA test with post hoc Dunnet tests. F(2) = 15.80. Istradefylline vs. istradefylline plus pramipexole: *$P = .0110$ and istradefylline plus pramipexole vs. istradefylline plus pramipexole plus CGS: $P > .99$), showing that Ca^{2+} currents restoration caused by A_{2A} receptors activation was blocked.

the Mutant Mouse Resource and Research Center at University of California at Davis, an NIH-funded strain repository, and was donated to the Mutant Mouse Resource and Research Center at University of California by Nathaniel Heintz, Ph.D., The Rockefeller University, GENSAT and Charles Gerfen, Ph.D., National Institutes of Health, National Institute of Mental Health. Mating was carried out between homozygous mice to obtain stable transgenic A_{2A}-Cre mice after breeding within a C57BL/6 background. Subjects were housed in acrylic cages (4–5 mice per cage; $19 \times 29 \times 12$ cm), and kept on a 12:12 light/dark period (light beginning at 8:00 am) in a temperature controlled, pathogen-free room allowed food and water *ad libitum*.

Experimental Procedures

To identify isolated iSPNs, A_{2A}-Cre mice at postnatal 25–45 were anesthetized i.p. with ketamine (Bayer 85 mg/kg) and xylazine (Bayer 15 mg/kg). Afterward, they were injected stereotaxically in a laminar flow hood (Telsar technologies, Model PV-30/60) in a dedicated sterile room with the following viral constructs (University of Pennsylvania Vector Core): AAV2/1.CAG.Flex.tdTomato.WPRE.bGH (Honguki Zeng) for whole-cell recordings in isolated cells. pAAV.Syn.Flex.GCaMP6f.WPRE.SV40 for calcium imaging recordings at the following coordinates relative to bregma (in mm): anteroposterior = 0.9, mediolateral = ±
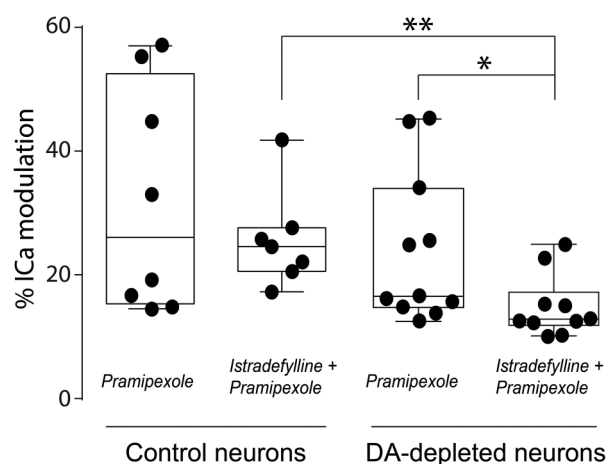
Figure 6. Blockade of A_{2A} receptors in dopamine-depleted neurons decreases D_2 receptor modulation. Box plots shows percentage modulation by pramipexole in different conditions. Pramipexole modulation is significantly less in dopamine-depleted neurons when istradefylline is present (n-pramipexole = 11 neurons from different slices and animals and n-pramipexole plus istradefylline = 10 neurons from different slices and animals; Mann-Whitney U test, F = 7.0, *P = .0127). In control neurons (non dopamine-depleted) pramipexole effect is not significantly different with or without istradefylline.

1.2, dorsoventral = − 3.2. The total virus volume injected was 0.6 μl over for 10 min to a 0.1 μl/min rate with a dental needle. After surgery, animals were monitored for two weeks to ensure protein expression and complete recovery. A total of 59 mice were used and randomly assigned to different experimental groups.

## Preparation of Acutely Dissociated Neurons and Brain Slices

Brain slices and acutely dissociated neurons were obtained as described in previous work (Duhne et al., 2021; Hernández-González et al., 2014; Rendon-Ochoa et al., 2018). Briefly, transfected A_{2A}-Cre mice were anesthetized (see above) and perfused intracardially with chilled sucrose solution (234 mM sucrose, 28 mM $NaHCO_3$, 7 mM dextrose, 4.54 mM pyruvate, 0.28 mM ascorbic acid, 2.5 mM KCl, 7 mM $MgCl_2$, 1.44 mM NaH_2PO_4, 0.4 mM $CaCl_2$, 4°C). For dopamine-depleted mice, there was a 14 days delay between rotational behavioral tests and calcium imaging experiments. Once brains were extracted, 300 μm thick sagittal slices were taken in a vibratome (1000 Classic, Warner Instruments, Hamden, USA) and kept in saline solution for 1 h at 34°C: 126 mM NaCl, 15 mM glucose, 26 mM $NaHCO_3$, 0.2 mM thiourea, 0.2 mM ascorbic acid, 2.5 mM KCl, 1.3 mM $MgCl_2$, 1.2 mM NaH_2PO_4 and 2.0 mM $CaCl_2$; pH = 7.4; 300 ± 5 mOsm/L continually perfused with 95% O_2 and 5% CO_2.

When recordings were done in slices, they were transferred to a submerged chamber and superfused at 5 ml/min with saline solution. For calcium imaging, slices were placed under a 20X immersion objective (Olympus XLUMPLFLN Objective, 1.00 numerical aperture, 2.0 mm width diameter) while constantly perfused with ACSF and 95% O_2 and 5% CO_2. When recordings were done in dissociated cells, the dorsal striatum was dissected from the slices and returned into the saline solution containing 10 mM HEPES plus 1 mg/ml of pronase E type XIV (Sigma-Aldrich, Mexico) at 34°C in for 15–20 min. After digestion, dissected striata were transferred to a low calcium saline solution (0.4 mM $CaCl_2$). To obtain acutely dissociated neurons, the tissue was mechanically dissociated with fire-polished Pasteur pipettes with different diameters. The cell suspension (1 ml) was placed into a Petri dish mounted on the stage of an inverted microscope (Nikon Instruments, Melville, NY, 20 ×/0.4 numerical aperture). Cells were left for 13 − 15 min to adhere to the bottom of the dish. The dish contained 1 ml of the whole-cell recording saline solution (in mM): 0.001 tetrodotoxin (TTX), 140 NaCl, 3 KCl, 5 $BaCl_2$, 2 $MgCl_2$, 10 HEPES, and 10 glucose (pH: 7.4 with NaOH; 300 ± 5-mOsm/l with glucose). Thereafter, the cells were superfused at 1 ml/min with saline of the same composition at room temperature (approximately 25–30°C). A_{2A} + neurons were visualized using an UV lamp (X-Cite; EXFO, Ontario, Canada). Dissociated neurons typically lack distal dendrites and prolonged axons (Supplementary Figure. 3A).

Voltage Clamp Recordings of Calcium Currents in Dissociated Neurons

Voltage-clamp recordings were performed on identified A_{2A} + neurons (Figure 1 and Supplementary Figure 3) with 8–15 μm diameter (Hernandez-Flores et al., 2015; Pérez-Burgos et al., 2010; Rendon-Ochoa et al., 2018). Patch pipettes of borosilicate glass (WPI, Sarasota, FL, USA) were pulled in a Flaming-Brown puller (Sutter instruments Corporation, Novato, CA, USA) and fire polished before use. For whole-cell recordings, electrodes with a D.C. resistance of 4–6 MΩ were used and liquid junctions potentials were corrected about 80%. Recordings were obtained with an Axopatch 200B patch-clamp amplifier (Axon instruments, Foster City, Ca, USA) and controlled and monitored using Im-Patch© (http://impatch.ifc.unam.mx/) an open access software (Lara-Gonzalez et al., 2019) and a 125 kHz DMA interface (Axon instruments). The internal solution contained (in mM): 180 N-methyl-d glucamine (NMDG), 40 HEPES, 10 EGTA, 4 $MgCl_2$, 2 ATP, 0.4 GTP and 0.1 leupeptin (pH = 7.2 with H_2SO_4; 280 ± 5 mOsm/l; room temperature around 25–30°C). We record and report Ca^{2+} currents using Ba^{2+} as a charge carrier as showed in previous articles (Bargas et al., 1994; Hernández-Flores et al., 2015; Hernández-González et al., 2014; Pérez-Burgos et al., 2010; Rendon-Ochoa et al., 2018). Ba^{2+} also serves as K^+ blocker and Na^+ channels were blocked with 1 μM of TTX.
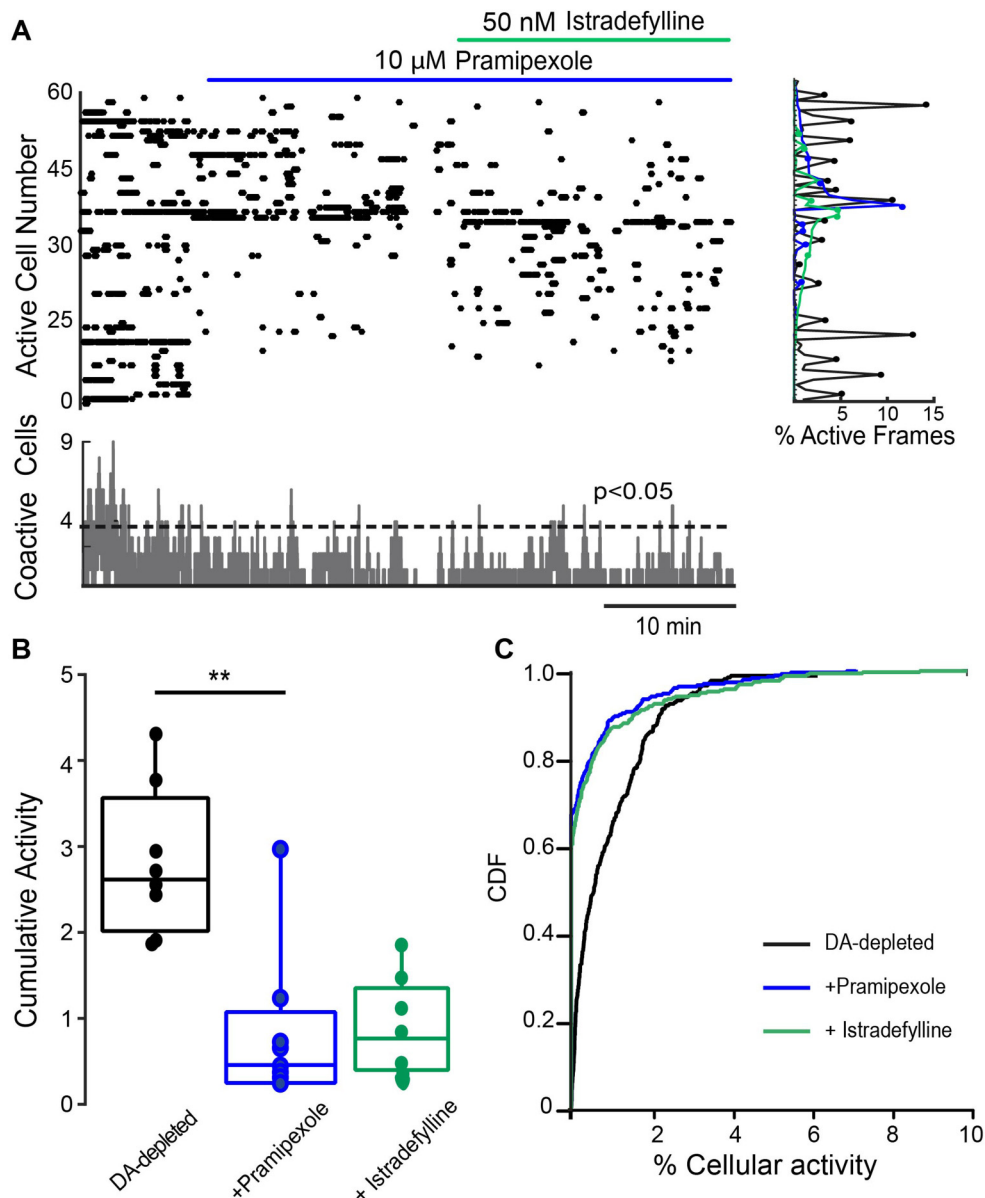
Figure 7. Interaction of pramipexole and istradefylline in the striatal parkinsonian circuit. A) Top: Representative raster plot where dots in rows represent the activity of indirect SPNs ($A_{2A}+$) along time as obtained with calcium imaging (see Methods). Three conditions are shown: first: an initial representative interval showing hyperexcitability of indirect SPNs proper of parkinsonism in a dopamine-depleted striatum (6-OHDA; Jaidar et al., 2019). Second: a reduction of this activity after activation of D_2 receptor by the dopamine-agonist pramipexole (blue bar; Lara-Gonzalez et al., 2019). Third: population activity does not change much when istradefylline is applied in the continuous presence of pramipexole (green bar). Histogram at right shows activity per row (active frames / total frames) in the different conditions denoted by colors. Histogram at bottom shows summed neuronal activity column by column (frame by frame). Dashed line is the threshold to detect significant peaks of coactivity. Note their reduction during both drugs. B) Box plots illustrate samples of cumulative activity (taken from cumulative activity -plots, see Methods) from raster plots taken at the three conditions: Activity during pramipexole is significantly reduced when compared to the parkinsonian condition (n = 8 from 8 different slices and 8 different animals, Friedman ANOVA test with post hoc Dunnet test. $F(2) = 9.75$ dopamine-depleted vs. pramipexole: $**P = .0081$). However, activity during pramipexole plus istradefylline was not significantly different to that of the control (dopamine-depleted vs. pramipexole plus istradefylline: $P = .0735$) showing that istradefylline reduced D_2 receptors action, in parallel to findings in single cells. Nonetheless, this reduction was not enough to return to the parkinsonian activity (istradefylline vs pramipexole plus istradefylline: $P = .9999$) supporting its therapeutic actions. C) Cumulative distribution functions of cellular activity in the three conditions (dopamine-depleted n1 = 273 neurons, pramipexole n2 = 103 neurons and pramipexole plus istradefylline n3 = 144 neurons; dopamine-depleted vs. pramipexole: $K = 0.67619$. $P = 2.8 \times 10^{-59}$; dopamine-depleted vs. pramipexole plus istradefylline: $K = 0.61264$. $P = 3.68 \times 10^{-52}$ and pramipexole vs. pramipexole plus istradefylline: $K = 0.071795$. $P = .33717$; Kolmogorov–Smirnov tests with the Benjamini–Hochberg method for False Discovery Rate).
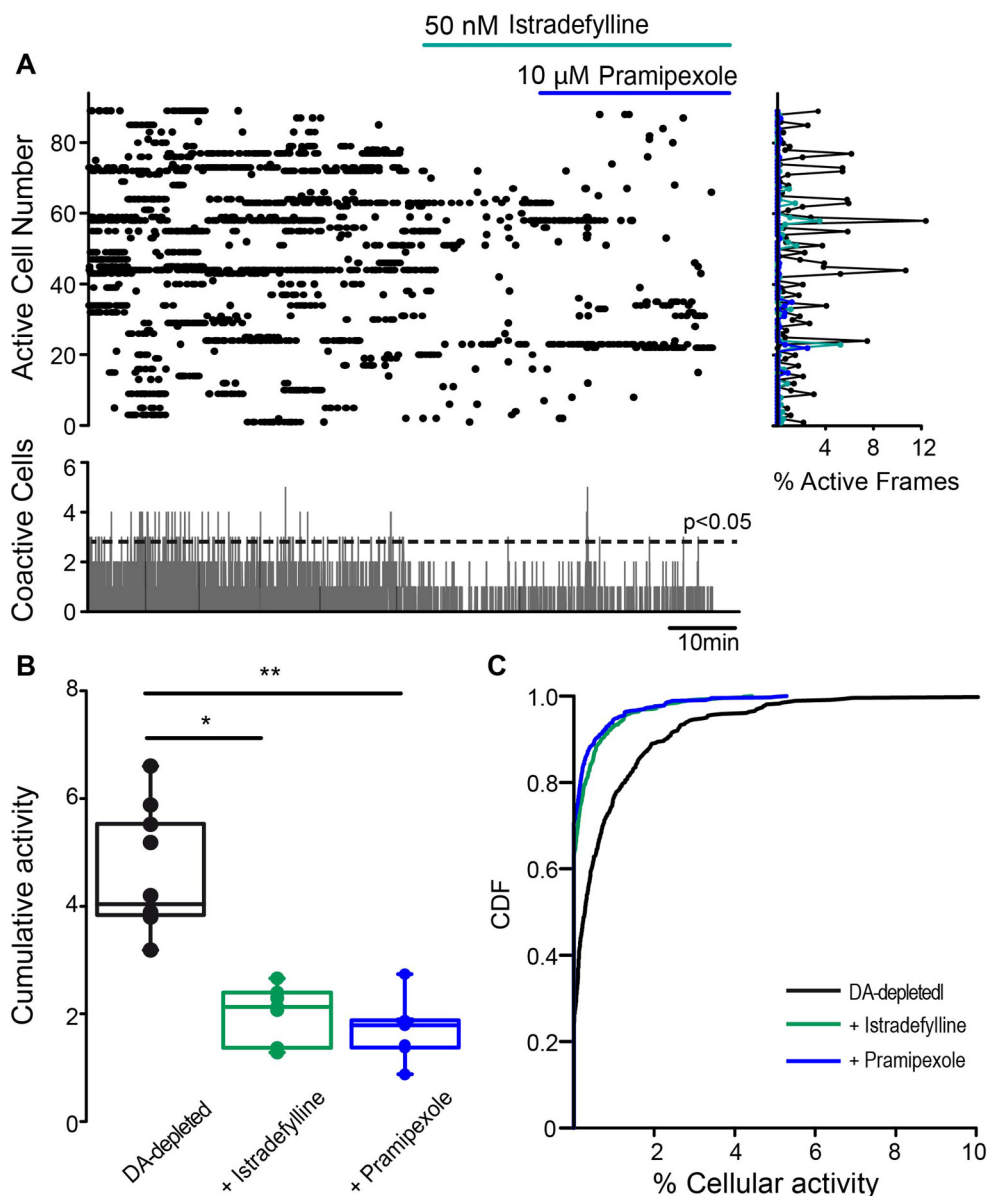
Figure 8. Istradefylline virtually occludes pramipexole modulation on indirect SPNs (A_{2A} +) activity in the striatal dopamine-depleted microcircuit. A) Raster plot: left, shows spontaneous hyperactivity of indirect SPNs in a dopamine-depleted microcircuit (6-OHDA model). Next, addition of 50 nM istradefylline (green bar) decreases indirect SPNs activity. Further application of 10 µM pramipexole in the continuous presence of istradefylline only shows a tendency for a small additional reduction of activity. Histogram at right shows activity row by row in all three conditions (denoted by colors). Histogram below shows the summed activity of active neurons at each movie frame. Dashed line in the histogram at bottom indicates the presence of statistically significant peaks of coactivity ($P < .01$), note their reduction during drugs application. B) Box plots compare slopes distributions of cumulative activity-plots (n = 8 from 8 different slices and animals, Friedman ANOVA with post hoc Dunnet test. $F(2) = 12.97$. dopamine-depleted vs. istradefylline: *$P = .022$; dopamine-depleted vs. istradefylline plus pramipexole: **$P = .0018$; istradefylline vs istradefylline plus pramipexole: $P = .830$). C) Cumulative distribution functions of % cellular activity of indirect SPNs in each condition (dopamine-depleted-$n_1 = 638$ neurons vs. istradefylline-$n_2 = 450$ neurons: $K = 0.38$. $P = 2.4 \times 10^{-36}$; dopamine-depleted vs. istradefylline plus pramipexole-$n_3 = 432$ neurons: $K = 0.38$. $P = 1.5 \times 10^{-51}$; pramipexole vs istradefylline plus pramipexole: $K = 0.079$. $P = .032$, from n = 8 from 8 different slices and 8 different animals; Kolmogorov-Smirnov test with the Benjamini–Hochberg method for a desired False Discovery Rate).

In this way, for simplicity, we will refer to Ba^{2+} currents as Ca^{2+} currents. Current-voltage relationships (I-V plots) were aquired before, during and after drug applications. Figure 1A shows a representative I-V plot evoked with 20 ms of rectangular voltage commands from −80 to 50 mV in 10 mV steps. In addition, Figure 1B shows the representative current in response to a voltage ramp command (0.7 mV/ms) from −80 to 50 mV. When I-V plots from

both methods coincided, space-clamp was considered acceptable (Figure 1C). For clarity, most figures only show representative reponses to voltage ramps. 200 μM Cd^{2+} completly blocked these currents (Figure 1D).

Current Clamp Recordings

Neurons were visualized using infrared differential interference contrast microscopy with an upright microscope and a digital camera. SPNs were identified using epifluorescent illumination (Supplementary Figure 3B). The signals were digitized at 10 kHz using an AT-MIO-16E4 board (National Instruments, Austin, TX, USA) and saved in a PC computer using Im-Patch©. Current-clamp recordings were performed with the patch clamp technique in the whole cell configuration in SPNs from the dorsal striatum, the membrane potential was held at -65 mV. Micropipettes were filled with internal saline (3–6 MΩ) containing (in mM): 115 KH_2PO_4, 2 $MgCl_2$, 10 HEPES, 1.1 EGTA, 0.2 ATP, 0.2 GTP, and 5% biocytin (pH = 7.2; 285 mOsm/L). Action potential firing was evoked by neuronal depolarizations (100 pA current pulses lasting 1000 ms) in control, in quinelorane (10 μM), and in quinelorane + CGS 21680 (1 μM). Digitized electrophysiological data were imported and analyzed using Origin (v.7, Microcal, Northampton, MA, USA; RIDD: rid_000069). We measured the action potential frequency of every evoked response and averaged the frequency of 15 responses for each neuron in every condition.

Calcium Imaging Experiments

Fluorophore stimulation was carried out with a Lambda HPX High power light emisor diode driver coupled to specific excitation emission filters. GCamp6f: excitation BP460–480 nm, emission 495–540 nm (Olympus, U-MGFPHQ). Imaging recordings were obtained with a CoolSnap K4 camera (Photometrics, Tucson, AZ, USA) and a Retiga R1 camera (Teledyne QImagingm, BC, Canadá), controlled by Im-Patch©. A_{2A} + neuron activity was observed using the GCaMP6f signal. Videos were 720–2160 frames long and acquisition rate was 6 frames / second. Noise was subtracted for both cameras since resolution is different (K4 2048 × 2048 resolution and Retiga 1360 × 1025 resolution). To cover long periods, 7–10 videos were taken per experiment, making up to 90 min per experiment. A 15 mM KCl solution was administered at the end of all experiments to test neuronal viability.

Videos were processed with ImPatch©, as previoulsy reported (Aparicio-Juaréz et al., 2019). Briefly, probability of firing action potentials during calcium transients was extracted as the first time derivative of the fluorescent signal (Carrillo-Reid et al., 2008). Then we built neuronal activity matrices were the y-axis denote active neurons and x-axis represent the sequence of movie frames as column vectors, transformed to time units. 1 denotes an active frame and 0 an inactive frame for each cell. Whole experiments can be contained in these matrices and expressed as raster plots, where each dot stands for a cell firing in that frame and each row shows the activity of a cell along time. The activity of all cells in all column frames was added to build coactivity histograms graphed below the raster plots. Significant coactivity peaks were determined using several variants of Montecarlo simulations with 10000 iterations each (Pérez-Ortega et al., 2016). Significant coactivity peaks can be observed in the frames in which the threshold was overcome (Supplementary Figure 4).

In this work we were interested in the amount of neuronal activity per experiment and this variable was quantified with cumulative activity plots (CA plots). CA plots plots were built by adding active raster columns along time (a sumatory of the coactivity histogram along time). To consider samples of experiments in the same condition, we used linear fits to CA plots (Lara-Gonzalez et al., 2019) (Supplementary Figure 1). Slopes of these fits from samples of neurons show whole neuronal activity during each experiment and their distribution was plotted as Tukey box plots (cumulative activity metrics). In this way we compared activity of samples of neurons in both control and during drugs applications. Samples using cumulative activity metrics were contrasted with Friedman ANOVA tests corrected for multiple comparisons using the Dunnet test.

The activity of individual cells through a single experiment was defined as the total number of active frames over the total number of frames, transformed to time units. This value, expressed as percentage of activity, was used to compare neuronal activity between different microcircuit conditions. To do that, cumulative distribution functions were plotted using all neurons from all samples from a given condition. Thus, cumulative distribution functions denote the probability or less that a given cell is active (P has values between 0 and 1). In this way distributions of neuronal populations were compared during different conditions. Cumulative distribution functions were contrasted with Kolmogorov-Smirnov tests corrected for multiple comparisons using the Benjamini-Hochberg procedure with a 0.05 FDR. The dopamine-depleted microcircuit is characterized by enhanced spontaneous activity (Jáidar et al., 2010; Pérez-Ortega et al., 2016). Note that CA plots and cumulative distribution functions are different metrics to measure the activity of the same neurons, in one case, various samples of experiments compared in different conditions are used as it is usually done. In the other case, probability distributions of neuronal activity using the set of all neurons taken from all experiments in the same condition are compared.

Electrophysiological Analysis

Digitized data were imported for analysis and plotted using commercial software (Origin 7, Microcal, Northampton, MA, USA). Mean ± SEM of peak Ca^{2+} currents for dissociated neurons and firing rate for current clamp recordings were reported. Free distributions were assumed, therefore, Friedman, Kruskal–Wallis or Wilcoxon test with post hoc Dunn or Dunnet tests for multiple comparisons were used

(signaled in each result). Friedman and Wilcoxon test were used when comparing the same samples in two or three different conditions (before, during and after application of a drug). $P < .05$ was used as significance threshold. Analysis was conducted by GraphPad Prism 6.01 (La Joya, CA).

Results

Habilitation of $A_{2A}R$ by D_2R in Isolated iSPNs from Dorsal striatum

To elucidate whether activation of adenosine $A_{2A}R$ requires a previous activation of D_2R in identified iSPNs from dorsal striatum we recorded isolated cells to avoid indirect effects. Figure 2A left shows a temporal course of the action of the $A_{2A}R$ selective agonist, CGS 21680 (CGS), on the maximal iCa^{2+} amplitude in an identified iSPNs: notably, bath application of 1 µM CGS alone had no significant effects on whole cell iCa^{2+} from isolated neurons (see also Supplementary Figure 2). iCa^{2+} amplitude went from 330 ± 56 pA in control (100%) to 315 ± 56 pA during application of the A_{2A} agonist ($95.3 \pm 2.4\%$; NS), suggesting that CGS cannot activate A_{2A} receptors by itself. Then, 10 µM pramipexole, a dopamine D_2R selective agonist, was applied: it reduced iCa^{2+} to 256 ± 49 ($22.83 \pm 3.9\%$), similar to results previously reported (Hernandez-Lopez et al., 2000). Thereafter, in the continuous presence of the D_2R agonist, pramipexole, a second application of CGS now increased and restored iCa^{2+} to nearly previous values: 311 ± 58 pA (increase of $26.7 \pm 5.9\%$), showing that $A_{2A}R$ are present and can be activated in iSPNs if enabled by the previous activation of D_2R, suggesting that the interaction between these receptors is necessary for $A_{2A}R$ activity, and also, a negative cooperativity or functional antagonism between both receptors on iCa^{2+}. This result parallels behavioral and biochemical antagonism previously reported (Ferré et al., 1991, 2008; Prasad et al., 2021; Preti et al., 2015; Stromberg et al., 2000; Yang et al., 1995). Figure 2A middle, shows representative I-V plots built from different moments during the time course denoted by numbers. Figure 2A right, summarize these results in samples of neurons using global linear slope measurements of cumulative activity metrics (see above and Supplementary Figure 1) graphed as box plots (n = 6 from different neurons and 6 different animals; Friedman ANOVA with post hoc Dunnet tests. F(3) = 12.60; control versus pramipexole: **$P = .004$; pramipexole versus pramipexole plus CGS: *$P = .04$), demonstrating that, after being enabled, $A_{2A}R$ activation counteracts the actions of D_2R.

Figure 2B shows that application of pramipexole or CGS produces no change on iCa^{2+} of a putative dSPN or A_{2a}-neuron (applied in any order; n = 6 from different neurons and 3 animals, Friedman ANOVA with post hoc Dunnet tests. F(2) = 4. $P = .1840$), suggesting that D_2-A_{2A} receptors interaction described above is proper of iSPNs and not present in dSPNs (Beggiato et al., 2014; Ferré et al., 2008).

Action of A_{2A} Receptors on Excitability

Neurons interconnected within their circuit may be the subject of multiple influences. Therefore, we wanted to observe if the activation of $A_{2A}R$ had an impact on neuronal excitability (Pérez-Garci et al., 2003) by counteracting D_2R activation, in non-isolated neurons. Therefore, current-clamp recordings from striatal slices were performed (Figure 3). We observed that, as expected (Hernandez-Lopez et al., 2000; Lara-Gonzalez et al., 2019), application of 10 µM quinelorane decreased frequency in iSPNs from 12.9 ± 0.63 Hz in control to 7.4 ± 0.8 Hz during D_2R activation (Figure 3 left and bottom, n = 8 neurons taken from 8 different slices and 8 different animals; Friedman ANOVA with post hoc Dunnet test. F(2) = 13.87. **$P = .0014$). The same effect can be obtained with different D_2R agonists (Lara-Gonzalez et al., 2019). Also note that the subsequent application of CGS partially restored firing frequency in iSPNs to 11 ± 0.56 Hz (*$P = .0374$ as compared with quinelorane alone).

We did not observe similar changes in firing frequency in putative dSPNs (A_{2A}-, Figure 3; right, n = 7 neurons from 7 different slices and 7 different animals, $P > .99$).

Istradefylline Shows Specificity of A_{2A} Receptors Actions: Differences Between Control and Dopamine-Depleted Mice

Next, we show that $A_{2A}R$ actions are specific, using isolated neurons and compared the D_2-A_{2A} receptors interaction without and with the presence of the $A_{2A}R$ antagonist, istradefylline, both in control and dopamine-depleted cells.

First, we show the actions in control (non dopamine-depleted) cells: 10 µM pramipexole decreased iCa^{2+} from 300 ± 55 pA to 185 ± 24 pA ($31.9 \pm 6.07\%$ decrease from control current), while subsequent administration of CGS counteracted this action by restoring iCa^{2+} amplitude to 255 ± 32 pA (an increase of $22.5 \pm 4.72\%$) in control neurons (Figure 4A; n = 8 from different neurons from 8 different animals; Friedman ANOVA with post hoc Dunnet tests. F(2) = 12.25. Control versus pramipexole: **$P = .0035$ and pramipexole versus pramipexole plus CGS: *$P = .0179$), confirming a significant recovery of iCa^{2+} by $A_{2A}R$ activation.

Similar experiments were done in the continuous presence of the $A_{2A}R$ antagonist istradefylline (Figure 4B): pramipexole had its usual reducing action of iCa^{2+} from 289 ± 69 pA to 234 ± 59 pA or $25.68 \pm 2.98\%$ (Figure 4B; n = 8 neurons taken from 8 different animals; Friedman ANOVA with post hoc Dunnet tests F(2) = 13.00. *$P = .0374$). However, the subsequent addition of CGS (in the continuous presence of pramipexole and istradefylline) had no the countertacting effect (compared with pramipexole alone: $P = .9521$ and compared to the control: **$P = .0014$), strongly suggesting that istradefylline was capable to block $A_{2A}R$ actions in spite of D_2R enabling effect in control cells (non dopamine-depleted neurons) and that these actions are, therefore, specific.

Next, we wanted to observe if this interaction was preserved in dopamine-depleted iSPNs and in case it was, whether it is found in the same amount. We used neurons taken from the injured side of the 6-OHDA rodent model of parkinsonism to test the habilitation of $A_{2A}R$ by D_2R. In isolated identified dopamine-depleted iSPNs, application of 10 μM pramipexole decreased iCa^{2+} from 323 ± 42 pA, to 236 ± 30 pA or $23.7 \pm 3.46\%$ showing that D_2R action on iCa^{2+} is preserved in dopamine-depleted cells (Prieto et al., 2009). During the continuous presence of pramipexole, addition of 1 μM CGS restored iCa^{2+} to 328 ± 37 pA, or $38 \pm 5.26\%$ (see box-plots in Figure 5A; n = 11 from different neurons from 10 different animals; Friedman ANOVA test with post hoc Dunnet tests F(2) = 16.55. Control versus pramipexole: $**P = .002$ and pramipexole versus pramipexole plus CGS: $***P = .0009$). These experiments confirmed, first, that in dopamine-depleted neurons D_2R activation reduces iCa^{2+} explaining its therapeutic actions (Lara-Gonzalez et al., 2019), and secondly, they show that the D_2-A_{2A} receptors interaction is present since D_2R activation habilitates $A_{2A}R$ activation to counteract the same D_2R actions that habilitated them on iCa^{2+}, in neurons from 6-OHDA injured mice, similarly as in neurons from control mice. Then we wanted to see whether istradefylline blocked these actions in dopamine-depleted iSPNs, an action that would further support its use as a therapeutic tool.

Therefore, we tested the ability of istradefylline to abolish $A_{2A}R$ restoration of iCa^{2+} in dopamine-depleted neurons. Figure 5B shows the effect of 10 μM pramiprexole in the continuous presence of 50 nM istradefylline: iCa^{2+} was decreased from 390 ± 100 pA to 333 ± 86 pA or $14.9 \pm 2.24\%$ in control neurons. Subsequent application of CGS in the continuous presence of pramipexole and istradefylline did not produce further changes in iCa^{2+} amplitude: 325 ± 82 pA showing that the effects were specific on $A_{2A}R$, supporting istradefylline role in maintaining a low excitability of iSPNs during parkinsonism and during the action of D_2R (n = 10 from different neurons from 9 different animals; Friedman ANOVA test with post hoc Dunnet tests F(2) = 15.80. Istradefylline versus istradefylline plus pramipexole: $*P = .0110$ and istradefylline plus pramipexole versus istradefylline plus pramipexole plus CGS: $P > .99$). Istradefylline impeded $A_{2A}R$ to restore iCa^{2+} in dopamine-depleted iSPNs after pramipexole action.

Notably however, when comparing non dopamine-depleted (control) with dopamine-depleted neurons from parkinsonian animals, pramipexole modulation appeared to be reduced in dopamine-depleted neurons when istradefylline was present (Bonaventura et al., 2015; Casadó-Anguera et al., 2016). Modulation was reduced from $25.7 \pm 3.0\%$ in control neurons versus 14.9 ± 2.2 in dopamine-depleted neurons, showing that D_2-A_{2A} receptors interaction goes both ways: the occupation of $A_{2A}R$ by an antagonist ligand reduced the modulatory action of a D_2R agonist during parkinsonism (Bonaventura et al., 2015; Casadó-Anguera,

2016; Prasad et al., 2021), these electrophysiological results support parallel biochemical actions that have been attributed to D_2-A_{2A} receptors oligomers and protein-protein interaction, that is, the non neutral action of A_{2A} receptor antagonists. By comparing percentages of iCa^{2+} modulation by pramipexole in control and dopamine-depleted neurons in the presence and absence of istradefylline (Figure 6) we found a decreased modulation by pramipexole in dopamine-depleted neurons when istradefylline was present (n-pramipexole = 11 neurons from different neurons from 10 different animals, n-pramipexole plus istradefylline = 10 neurons from different neurons from 9 different animals; Mann-Whitney U test, F = 7.0, $*P = .0127$). In control iSPNs, pramipexole modulation showed no significant differences with or without istradefylline. However, istradefylline seemed to decrease the variance in both samples (Figure 6). These results are a molecular correlate of D_2-A_{2A} receptors interaction in dopamine-depleted iSPNs (Ferré et al., 2008). Because this change in D_2R modulation of iCa^{2+} was present in dopamine-depleted neurons we decided to evaluate the global impact of the D_2-A_{2A} receptors interaction in dopamine-depleted neuronal populations in ex-vivo striatal parkinsonian tissue by using Ca^{2+} imaging with single cell resolution.

Pramipexole and Istradefylline Interaction depends on the Order of Drugs Administration in the Striatal Circuitry

We focused in the spontaneous hyperexcitability of identified iSPNs due to dopamine-depletion (A_{2A} + neurons; Figure 7A left; Jáidar et al., 2010, 2019; Plata et al., 2013). Bath application of 10 μM of pramipexole reduced iSPNs activity as reported before in the whole circuit (Lara-González et al., 2019; Figure 7A blue bar). Under these conditions, a subsequent administration of istradefylline in the continuous presence of pramipexole, failed to further decrease neuronal activity but did not restore parkinsonian activity significantly (Figure 7A green bar). Histogram of coactivity (Figure 7A bottom) shows a reduction of significant coactivity peaks and less activity during pramiprexole application. The addition of istradefylline caused a small reduction of pramipexole effects, in parallel with single cell experiments. Box plots (Figure 7B) summarize these results (n = 8 experiments from 8 differents slices and 8 different animals, Friedman ANOVA test with post hoc Dunnet test. F(2) = 9.75. dopamine-depleted versus pramipexole: $**P = .0081$; dopamine-depleted versus pramipexole plus istradefylline: $P = .0735$; pramipexole versus pramipexole plus istradefylline: $P = .9999$).

Figure 7C shows cumulative distribution functions of cellular activity in the three conditions by taking all the neurons in each condition (dopamine-depleted-n1 = 273 neurons, pramipexole-n2 = 103 neurons and pramipexole plus istradefylline-n3 = 144 neurons. dopamine-depleted vs.

pramipexole: $K = 0.67619$, $P = 2.8091 \times 10^{-59}$; dopamine-depleted vs. pramipexole plus istradefylline: $K = 0.61264$. $P = 3.6841 \times 10^{-52}$. Pramipexole vs. pramipexole plus istradefylline: $K = 0.071795$, $P = .33717$; Kolmogorov–Smirnov test with the Benjamini–Hochberg method for a desired false discovery rate). That is, at the global circuit level, addition of istradefylline did not appear to interfere much with pramipexole anti-parkinsonian activity: only a few more neurons were activated after its addition when counting all recorded neurons from all experimental samples (Figure 7A and B); at a larger scale other influences present in the tissue may intervene (cumulative distribution functions in Figure 7C; see Discussion). These results support the use of istradefylline in therapeutics in spite of the reduction in D_2R action.

Nevertheless, the order of drugs administration appears to influence D_2-A_{2A} receptors interaction in DA-depleted ex-vivo tissue: Figure 8A raster plot (left) shows an initial and representative period of the spontaneous hyperactivity of iSPNs present in dopamine-depleted tissue. Unexpectedly, 50 nM istradefylline administered alone decreased parkinsonian striatal activity in a significant amount (Figure 8A green bar) observed as less active neurons and a reduction in significant peaks of coactivity (Figure 7A and B). A subsequent application of pramipexole further tended to decrease the activity by a very small (non-significant) amount (Figure 8A blue bar, see below), showing that istradefylline virtually occluded the dopamine-agonist effect. Figure 8B show a box plot summary of cumulative activity plot samples comparisons in the different conditions (n = 8 experiments from 8 different slices from 8 differents animals, Friedman ANOVA with post hoc Dunnet test. $F(2) = 12.97$. dopamine-depleted versus istrasdefylline: *$P = .022$ was significant, contrary to the lack of significance when istradefylline was applied after pramipexole (Figure 7A and B); dopamine-depleted versus istradefylline plus pramipexole: **$P = .0018$; istradefylline versus istradefylline plus pramipexole: $P = .830$). Figure 8C shows cumulative distribution functions of cellular activity for all iSPNs taken from all experiments in the different conditions (n = 8 experiments from 8 different slices and 8 different animals: dopamine-depleted-n1 = 638 neurons vs. istradefylline-n2 = 450 neurons: $K = 0.38$. $P = 2.4017 \times 10^{-36}$; dopamine-depleted vs. istradefylline plus pramipexole-n3 = 432 neurons: $K = 0.38$. $P = 1.5061 \times 10^{-51}$ and pramipexole vs. istradefylline plus pramipexole: $K = 0.079$. $P = .032$; Kolmogorov-Smirnov tests with the Benjamini–Hochberg method for a false discovery rate).

Discussion

Focusing on iCa^{2+} and excitability as indicators of D_2-A_{2A} receptors interactions, future work will investigate the classes of Ca^{2+} channel involved (Bargas et al., 1994; Rendón-Ochoa et al., 2018). The main findings of this work are: 1) $A_{2A}R$ do not modulate iCa^{2+} currents by themselves in iSPNs, they need the previous activation of D_2R,

confirming an interaction that enables $A_{2A}R$ actions in iSPNs. 2) This interaction resulted to be antagonistic: previous D_2R activation as evaluated by a reduction in iCa^{2+}, habilitates $A_{2A}R$ to counteract D_2R actions on iCa^{2+} in dissociated iSPNs, as evaluated by a recovery in the current reduced by D_2R action. That is: $A_{2A}R$ were enabled by D_2R to oppose their actions. These electrophysiological results parallels previously biochemical antagonistic interactions reported between both receptors. 3) Brain slice experiments were consistent with these findings, as evaluated by neuronal excitability: D_2R first decreased firing frequency and then $A_{2A}R$ restored it. 4) The interaction of D_2-A_{2A} receptors is preserved in dopamine-depleted iSPNs, using the 6-OHDA PD model, 5) Istradefylline blocked the action of $A_{2A}R$ in both control and dopamine-depleted iSPNs, demonstrating specificity, 6) Istradefylline decreased the modulation on iCa^{2+} by D_2R in dopamine-depleted cells, showing that the interaction goes both ways, in parallel with previously reported decrease in D_2R actions by $A_{2A}R$ occupation. 7) Istradefylline failed to further reduce iSPNs activity while comparing samples of iSPNs previously treated with pramipexole, in fact, the number of active cells slightly increased. However, the tissue did not return to parkinsonian activity, and in a larger sample used to build cumulative distribution functions it is shown that istradefylline does not significantly interfere with the dopamine-agonist action, supporting their coadjuvant effect in therapy. 8) When administered before, istradefylline, reduced parkinsonian hyperactivity by a significant amount, virtually occluding the subsequent action of pramipexole, which had only a tendency to a marginal additional activity.

D_2-A_{2A} Receptors Antagonistic Interaction on Ca^{2+} Channels Modulation in iSNPs

A D_2-A_{2A} receptors interaction was demonstrated by the fact that in acutely dissociated iSPNs, free from additional interferences, $A_{2A}R$ do not modulate iCa^{2+} by themselves. They need habilitation by a previous activation of D_2R. As previously reported with pharmacological and biochemical studies (Fuxe et al., 2010; Hillion et al., 2002; Sheth et al., 2014), the D_2-A_{2A} receptors interaction resulted to be antagonistic: previous D_2R activation showed a reduction in iCa^{2+} and the habilitation of $A_{2A}R$ in turn opposed or counteracted D_2R action by recovering iCa^{2+} thus paralleling previously reported biochemical interactions (Ferré et al., 1991, 2008; Stromberg et al., 2000; Yang et al., 1995). In addition, brain slice experiments demonstrate that actions on excitability due to activation of $A_{2A}R$ after activation of D_2R can be observed in iSPNs recorded in slices: D_2R actions decreased firing frequency (Hernandez-Lopez et al., 2000; Lara-Gonzalez et al., 2019) and then $A_{2A}R$ actions restored it reversing the decrease in firing due to D_2R, similarly to results obtained in nucleus accumbens (Azdad et al., 2009)

where Ca^{2+} channels and membrane to membrane interactions between both receptors are thought to be involved.

Istradefylline blocked the action of $A_{2A}R$ in both control and dopamine-depleted iSPNs, demonstrating specificity (Mizuno et al., 2010; Muller, 2015; Preti et al., 2015; Richardson et al., 1997). in its presence, CGS failed to recover or enhance iCa^{2+} proving that $A_{2A}R$ was responsible for current enhancement. Furthermore, they confirmed that changes in excitability run in parallel to those in iCa^{2+} (Hernandez-Flores et al., 2015; Hernandez-Gonzalez et al., 2014; Pérez-Garci et al., 2003; Rendon-Ochoa et al., 2018; Vilchis et al., 2002), validating iCa^{2+} carried by Ca^{2+} channels as a molecular effector to test D_2-A_{2A} interactions.

Although istradefylline successfully blocked CGS actions, it is notable that D_2R modulation decreased in neurons taken from the 6-OHDA model, since in intact mice there are no significant differences between D_2R modulation with or without istradefylline: istradefylline decreased the modulation on iCa^{2+} by D_2R, showing that the D_2-A_{2A} interaction goes both ways, in parallel with previously reported decrease in D_2R actions by $A_{2A}R$ occupation (Bonaventura et al., 2015; Prasad et al., 2021; Stromberg et al., 2000). It has been reported that concentrations of 0.1 to 3 mM of caffeine, a non selective antagonist and the selective antagonists SCH 58261 and KW 6002 decreased D_2 modulation in membrane preparations of sheep striatum with radioligand experiments (Bonaventura et al., 2015). These results suggest that the occupancy of the antagonist or agonist in the $A_{2A}R$ produces some kind of change in the D_2R, reducing its affinity. One hypothesis stands that $A_{2A}R$ agonists or antagonists decreases intrinsic efficacy of any D_2R ligand in a orthosteric fashion because the integrity of the D_2-A_{2A} receptors oligomer is affected (Azdad et al., 2009; Bonaventura et al., 2015). Although, it is not the objective of this work to elucidate the existence of heteromers, our results support this hypothesis (Prasad et al., 2021) that is still debated (Fredholm et al., 2011).

Istradefylline failed to further reduce iSPNs activity while comparing samples of iSPNs previously treated with pramipexole, in fact, the number of active cells slightly increased, as though implying a reduction in pramipexole effects, however, parkinsonian activity did not return (Prasad et al., 2021). These results support the hypothesis that istradefylline may be a good coadjuvant to L-DOPA therapy since it would not allow the increase in excitability caused by iCa^{2+} restoration induced by $A_{2A}R$ activation at the population level.

When Applied First Istradefylline Occludes Pramiprexole iCa^{2+} Modulation When Observed in Neuronal Populations

To evaluate the impact of istradefylline during dopamine-agonist actions found in samples of dopamine-depleted single neurons, and to extrapolate these findings to the parkinsonian tissue itself, we used the simultaneous recordings of dozens of neurons with Ca^{2+} imaging in striatal brain slices from 6-OHDA mice. The microcircuit behavior of the parkinsonian microcircuit has been reported elsewhere (Perez-Ortega et al. 2016). Here we were mainly interested in whole neuronal activity. We used a genetically coded indicator of Ca^{2+} influx: virally transfected GCaMP6f (see Materials and methods and Supplementary Figure 3), that allows record various identified neurons with single cell resolution (Aparicio-Juarez et al., 2019; Duhne et al., 2021). In these conditions, the parkinsonian circuitry is characterized by hyperactivity followed by the appearance of multiple peaks of coactivity and a highly recurrent neuronal ensemble (Jáidar et al., 2010, 2019; Lara-Gonzalez et al., 2019; Plata et al., 2013). It is also known that adenosine levels in the tissue are correlated with neuronal activity (Prasad et al., 2021).

Istradefylline failed to further significantly reduce iSPNs hyperactivity while comparing samples of iSPNs previously treated with pramipexole, in fact, the number of active cells slightly increased. However, the tissue did not return to parkinsonian activity, and in the larger sample used to build cumulative distribution functions it is shown that istradefylline does not significantly interfere with the dopamine-agonist action, supporting their coadjuvant effect in therapy.

In addition, when administered before, istradefylline, reduced parkinsonian hyperactivity by a significant amount, virtually occluding the subsequent action of pramipexole, which had only a tendency to a marginal additional activity. It is known that istradefylline combined with low doses of L-DOPA, enhances anti-parkinsonian activity in MPTP marmosets (Uchida et al., 2015) and in clinical trials (Bara-Jimenez et al., 2003; Hauser et al., 2011; Kondo et al., 2015; LeWitt & Fahn, 2016). The dopamine-agonist had a negligible effect when added after istradefylline, probably due to the reducing action of D_2R activation by $A_{2A}R$ blockade. But the joint action of these drugs seems to be efficient to disminish microcircuit hyperactivity during parkinsonism, supporting the coadjuvant effects of $A_{2A}R$ blockade.

Discrepancies between samples of single cells and measures with larger samples at a greater scale may be explained by additional interferences: for example, a D_2-A_{2A} receptors interaction is involved in glutamate release by glial cells (Cervetto et al., 2017), in controlling corticostriatal transmission (Tozzi et al., 2007), the excitability of cholinergic interneurons (Tozzi et al., 2011) and $A_{2A}R$ are also habilitated by A_1 receptors (Hernandez-Gonzalez et al., 2014) whose activation depends on adenosine concentration which in turn depends on neuronal activity which is high during parkinsonism.

In this work, we provided evidence that Ca^{2+} channels are molecular effectors of the well known D_2-A_{2A} receptors antagonistic interaction reported in several pharmacological tests in the dorsal striatum of mice (Prasad et al., 2021), including the reported antagonist actions of $A_{2A}R$ onto D_2R function on iSPNs (Ferré et al., 2008; Stromberg et al.,

2000), adding evidence that D_2-A_{2A} interaction goes both ways and showing the efficacy of $A_{2A}R$ blockade as an adjuvant in anti-pakinsonian therapy. Habilitation of $A_{2A}R$ to modulate iCa^{2+} was previously shown with adenosine A_1 receptors (Hernandez-Gonzalez et al., 2014), suggesting that other receptors, out of the scope of the present work and in need of further investigation, may be able to habilitate $A_{2A}R$ in iSPNs. When tested in samples of single neurons, $A_{2A}R$ blockade appears to interfere with the action of D_2R, however, this effect was of little importance when looking at larger neuronal populations, highlighting the possible differences found between samples of a few neurons and larger samples in parkinsonian tissue subject to several influences. However, to elucidate whether these actions are due to allosteric protein-protein interactions or at the level of signaling cross-talk is out of the scope of the present work (Casadó-Anguera et al., 2016; Fernandez-Dueñas et al., 2019). Notwithstanding, these experiments open the question about what is the role of Ca^{2+} channels in the possible heteromers that may be participating. In sum, the present electrophysiological findings support the hypotheses previously found with biochemical work: that $A_{2A}R$-D_2R heteromers may exhibit negative allosteric protein-protein interactions: $A_{2A}R$ agonists counteracting the action of D_2R agonists (and vice versa) and that $A_{2A}R$ antagonists not only block the action of $A_{2A}R$ agonists but also reduce the modulatory action of D_2R agonists.

Author Contribution

EAR-O: Conceptualization, Methodology, Formal analysis, Investigation, Data Curation, Writing - Original Draft, Writing - Review & Editing, Visualization; TH-F: Investigation, Writing - Review & Editing; MP-O: Methodology, Software, Investigation, Resources, Writing - Original Draft, Writing - Review & Editing, Visualization; MBP-R: Methodology, Investigation, Writing - Original Draft, Writing - Review & Editing, Visualization; VHA-R: Methodology, Investigation, Writing - Review & Editing; VMC: Methodology, Software, Investigation, Writing - Original Draft, Writing - Review & Editing, Visualization; OH-G: Investigation; MP-R: Methodology, Resources; EG: Conceptualization, Methodology, Project administration, Funding acquisition, Supervision, Writing - Review & Editing; JB: Conceptualization, Methodology, Project administration, Funding acquisition, Supervision, Writing - Review & Editing

Declaration of Conflicting Interests

The author(s) declared no potential conflicts of interest with respect to the research, authorship, and/or publication of this article.

Funding

ORCID iDs

Vladimir Melesio Calderon [ID] https://orcid.org/0000-0002-4376-6677
José Bargas [ID] https://orcid.org/0000-0002-8205-8163

Supplemental material

Supplemental material for this article is available online.

References

Aparicio-Juárez, A., Duhne, M., Lara-González, E., Ávila-Cascajares, F., Calderón, V., Galarraga, E., & Bargas, J. (2019). Cortical stimulation relieves parkinsonian pathological activity in vitro. *European Journal of Neuroscience*, *49*(6), 834–848. https://doi.org/10.1111/ejn.13806.

Armentero, M. T., Pinna, A., Ferré, S., Lanciego, J. L., Müller, C. E., & Franco, R. (2011). Past, present and future of A(2A) adenosine receptor antagonists in the therapy of Parkinson's disease. *Pharmacology & Therapeutics*, *132*(3), 280–299. https://doi.org/10.1016/j.pharmthera.2011.07.004

Azdad, K., Gall, D., Woods, A. S., Ledent, C., Ferre, S., & Schiffmann, S. N. (2009). Dopamine D2 and adenosine A2A receptor regulate NMDA-mediated excitation in accumbens neurons through A2A – D2 receptor heteromerization. *Neuropsychopharmacology*, *34*(4), 972–986. https://doi.org/10.1038/npp.2008.144

Bara-Jimenez, W., Sherzai, A., Dimitrova, T., Favit, A., Bibbiani, F., Gillespie, M., Morris, M. J., Mouradian, M. M., & Chase, T. N. (2003). Adenosine A(2A) receptor antagonist treatment of Parkinson's disease. *Neurology*, *61*(3), 293–296. https://doi.org/10.1212/01.WNL.0000073136.00548.D4

Bargas, J., Howe, A., Eberwine, J., Cao, Y., & Surmeier, D. J. (1994). Cellular and molecular characterization of Ca^{2+} currents in acutely isolated, adult rat neostriatal neurons. *The Journal of Neuroscience*, *14*(11), 6667–6686. https://doi.org/10.1523/JNEUROSCI.14-11-06667.1994

Beggiato, S., Antonelli, T., Tomasini, M. C., Borelli, A. C., Agnati, L. F., Tanganelli, S., Fuxe, K., & Ferraro, L. (2014). Adenosine A2A-D2 receptor-receptor interactions in putative heteromers in the regulation of the striato-pallidal gaba pathway: Possible relevance for Parkinson's disease and its treatment. *Current Protein & Peptide Science*, *15*(7), 673–680. https://doi.org/10.2174/1389203715666140901103205.

Berthet, A., & Bezard, E. (2009). Dopamine receptors and L-dopa-induced dyskinesia. *Parkinsonism & Related Disorders*, *15*(Suppl 4), 8–12. https://doi.org/10.1016/S1353-8020(09)70827-2

Bonaventura, J., Navarro, G., Casadó-Anguera, V., Azdad, K., Rea, W., Moreno, E., Brugarolas, M., Mallol, J., Canela, E. I., Lluís, C., Cortés, A., Volkow, N. D., Schiffmann, S. N., Ferré, S., & Casadó, V. (2015). Allosteric interactions between agonists and antagonists within the adenosine A2A receptor-dopamine D2 receptor heterotetramer. *Proceedings of the National Academy of Sciences of the United States of America*, *112*(27), E3609–E3618. https://doi.org/10.1073/pnas.1507704112

Bové, J., Marin, C., Bonastre, M., & Tolosa, E. (2002). Adenosine A2A antagonism reverses levodopa-induced motor alterations in hemiparkinsonian rats. *Synapse (New York, N.Y.)*, *46*(4), 251–257. https://doi.org/10.1002/syn.10112

Carrillo-Reid, L., Tecuapetla, F., Tapia, D., Hernández-Cruz, A., Galarraga, E., Drucker-Colin, R., & Bargas, J. (2008). Encoding network states by striatal cell assemblies. *Journal of Neurophysiology*, *99*(3), 1435–1450. https://doi.org/10.1152/jn.01131.2007

Casadó-Anguera, V., Bonaventura, J., Moreno, E., Navarro, G., Cortés, A., Ferré, S., & Casadó, V. (2016). Evidence for the heterotetrameric structure of the adenosine A2A-dopamine D2 receptor complex. *Biochemical Society Transactions*, *44*(2), 595–600. https://doi.org/10.1042/BST20150276

Cervetto, C., Venturini, A., Passalacqua, M., Guidolin, D., Genedani, S., Fuxe, K., Borroto-Esquela, D. O., Cortelli, P., Woods, A., Maura, G., Marcoli, M., & Agnati, L. F. (2017). A2A-D2 receptor-receptor interaction modulates gliotransmitter release from striatal astrocyte processes. *Journal of Neurochemistry*, *140*(2), 268–279. https://doi.org/10.1111/jnc.13885.

Duhne, M., Lara-González, E., Laville, A., Padilla-Orozco, M., Ávila-Cascajares, F., Arias-García, M., Galarraga, E., & Bargas, J. (2021). Activation of parvalbumin-expressing neurons reconfigures neuronal ensembles in murine striatal microcircuits. *European Journal of Neuroscience*, *53*(7), 2149–2164. https://doi.org/10.1111/ejn.14670

Fernández-Dueñas, V., Gómez-Soler, M., Valle-León, M., Watanabe, M., Ferrer, I., & Ciruela, F. (2019). Revealing adenosine A_{2A}-dopamine D_2 receptor heteromers in Parkinson's disease post-mortem brain through a new AlphaScreen-based assay. *International Journal of Molecular Sciences*, *20*(14), 3600. https://doi.org/10.3390/ijms20143600

Ferré, S., & Fuxe, K. (1992). Dopamine denervation leads to an increase in the intramembrane interaction between adenosine A2 and dopamine D2 receptors in the neostriatum. *Brain Research*, *594*(1), 124–130. https://doi.org/10.1016/0006-8993(92)91036-e.

Ferré, S., Herrera-Marschitz, M., Grabowska-Andén, M., Ungerstedt, U., Casas, M., & Andén, N. E., & Postsynaptic dopamine/adenosine interaction: I. (1991). Adenosine analogues inhibit dopamine D2-mediated behaviour in short-term reserpinized mice. *European Journal of Pharmacology*, *192*(1), 25–30. https://doi.org/10.1016/0014-2999(91)90064-w.

Ferré, S., Quiroz, C., Woods, A. S., Cunha, R., Popoli, P., Ciruela, F., Lluis, C., Franco, R., Azdad, K., & Schiffmann, S. N. (2008). An update on adenosine A2A-dopamine D2 receptor interactions: Implications for the function of G protein-coupled receptors. *Current Pharmaceutical Design*, *14*(15), 1468–1474. https://doi.org/10.2174/138161208784480108.

Floran, B., Gonzalez, B., Florán, L., Erlij, D., & Aceves, J. (2005). Interactions between adenosine A(2a) and dopamine D2 receptors in the control of [(3)H]GABA release in the globus pallidus of the rat. *European Journal of Pharmacology*, *520*(1-3), 43–50. https://doi.org/10.1016/j.ejphar.2005.06.035

Fredholm, B. B., Arslan, G., Halldner, L., Kull, B., Schulte, G., & Wasserman, W. (2000). Structure and function of adenosine receptors and their genes. *Naunyn-Schmiedeberg's Archives of Pharmacology*, *362*(4–5): 364–374. https://doi.org/10.1007/s002100000313.

Fredholm, B. B., IJzerman, A. P., Jacobson, K. A., Linden, J., & Müller, C. E. (2011). International union of basic and clinical pharmacology. LXXXI. Nomenclature and classification of adenosine receptors--an update. *Pharmacological Reviews*, *63*(1), 1–34. https://doi.org/10.1124/pr.110.003285.

Fuxe, K., Marcellino, D., Leo, G., & Agnati, L. F. (2010). Molecular integration via allosteric interactions in receptor heteromers. A working hypothesis. *Current Opinion in Pharmacology*, *10*(1), 14–22. https://doi.org/10.1016/j.coph.2009.10.010.

Hauser, R. A., Ellenbogen, A. L., Metman, L. V., Hsu, A., O'Connell, M. J., Modi, N. B., Yao, H. M., Kell, S. H., & Gupta, S. K. (2011). Crossover comparison of IPX066 and a standard levodopa formulation in advanced Parkinson's disease. *Movement Disorders*, *26*(12), 2246–2252. https://doi.org/10.1002/mds.23861

Hernández-Flores, T., Hernández-González, O., Pérez-Ramírez, M. B., Lara-González, E., Arias-García, M. A., Duhne, M., Pérez-Burgos, A., Prieto, G. A., Figueroa, A., Galarraga, E., & Bargas, J. (2015). Modulation of direct pathway striatal projection neurons by muscarinic M_4-type receptors. *Neuropharmacology*, *89*, 232–244. https://doi.org/10.1016/j.neuropharm.2014.09.028

Hernández-González, O., Hernández-Flores, T., Prieto, G. A., Pérez-Burgos, A., Arias-García, M. A., Galarraga, E., & Bargas, J. (2014). Modulation of Ca2 + -currents by sequential and simultaneous activation of adenosine A1 and A2A receptors in striatal projection neurons. *Purinergic Signalling*, *10*, 269–281. https://doi.org/10.1007/s11302-013-9386-z

Hernández-López, S., Bargas, J., Surmeier, D. J., Reyes, A., & Galarraga, E. (1997). D1 receptor activation enhances evoked discharge in neostriatal medium spiny neurons by modulating an L-type Ca2 + conductance. *The Journal of Neuroscience*, *17*(9), 3334–3342. https://doi.org/10.1523/JNEUROSCI.17-09-03334.1997

Hernandez-Lopez, S., Tkatch, T., Perez-Garci, E., Galarraga, E., Bargas, J., Hamm, H., & Surmeier, D. J. (2000). D2 dopamine receptors in striatal medium spiny neurons reduce L-type Ca2 + currents and excitability via a novel PLC[beta]1-IP3-calcineurin-signaling cascade. *The Journal of Neuroscience*, *20*(24), 8987–8995. https://doi.org/10.1523/JNEUROSCI.20-24-08987.2000.

Hillion, J., Canals, M., Torvinen, M., Casado, V., Scott, R., Terasmaa, A., Hansson, A., Watson, S., Olah, M. E., Mallol, J., Canela, E. I., Zoli, M., Agnati, L. F., Ibanez, C. F., Lluis, C., Franco, R., Ferre, S., & Fuxe, K. (2002). Coaggregation, cointernalization, and codesensitization of adenosine A2A receptors and dopamine D2 receptors. *Journal of Biological Chemistry*, *277*(20), 18091–18097. https://doi.org/10.1074/jbc.M1077312007.

Jacobson, K. A., & Gao, Z. G. (2006). Adenosine receptors as therapeutic targets. *Nature Reviews Drug Discovery*, *5*(3), 247–264. https://doi.org/10.1038/nrd1983

Jáidar, O., Carrillo-Reid, L., Hernández, A., Drucker-Colín, R., Bargas, J., & Hernández-Cruz, A. (2010). Dynamics of the parkinsonian striatal microcircuit: Entrainment into a dominant network state. *Journal of Neuroscience*, *30*(34), 11326–11336. https://doi.org/10.1523/JNEUROSCI.1380-10.2010.

Jáidar, O., Carrillo-Reid, L., Nakano, Y., Lopez-Huerta, V. G., Hernandez-Cruz, A., Bargas, J., Garcia-Munoz, M., & Arbuthnott, G. W. (2019). Synchronized activation of striatal direct and indirect pathways underlies the behavior in unilateral dopamine-depleted mice. *The European Journal of Neuroscience*, *49*(11), 1512–1528. https://doi.org/10.1111/ejn.14344

Ko, W., Camus, S. M., Li, Q., Yang, J., McGuire, S., Pioli, E. Y., & Bezard, E. (2016). An evaluation of istradefylline treatment on parkinsonian motor and cognitive deficits in 1–methyl-4-phenyl-1,2,3,6-tetrahydropyridine (MPTP)-treated macaque models. *Neuropharmacology*, *110*(Pt A), 48–58. https://doi.org/10.1016/j.neuropharm.2016.07.012

Kondo, T., & Mizuno, Y., & Japanese Istradefylline Study Group (2015). A long-term study of istradefylline safety and efficacy in patients with Parkinson disease. *Clinical*

Neuropharmacology, *38*(2), 41–46. https://doi.org/10.1097/WNF.0000000000000073

Kravitz, A. V., Freeze, B. S., Parker, P. R., Kay, K., Thwin, M. T., Deisseroth, K., & Kreitzer, A. C. (2010). Regulation of parkinsonian motor behaviours by optogenetic control of basal ganglia circuitry. *Nature*, *466*(7306), 622–626. https://doi.org/10.1038/nature09159

Lara-González, E., Duhne, M., Ávila-Cascajares, F., Cruz, S., & Bargas, J. (2019). Comparison of actions between L-DOPA and different dopamine agonists in striatal DA-depleted microcircuits in vitro: Pre-clinical insights. *Neuroscience*, *410*, 76–96. https://doi.org/10.1016/j.neuroscience.2019.04.058

Lewitt, P. A. (2008). Levodopa for the treatment of Parkinson's disease. *The New England Journal of Medicine*, *359*(23), 2468–2476. https://doi.org/10.1056/NEJMct0800326

LeWitt, P. A., & Fahn, S. (2016). Levodopa therapy for Parkinson disease: A look backward and forward. *Neurology*, *86*(14 Suppl 1), S3–S12. https://doi.org/10.1212/WNL.0000000000002509

Matsuya, T., Takuma, K., Sato, K., Asai, M., Murakami, Y., Miyoshi, S., Noda, A., Nagai, T., Mizoguchi, H., Nishimura, S., & Yamada, K. (2007). Synergistic effects of adenosine A2A antagonist and L-DOPA on rotational behaviors in 6-hydroxydopamine-induced HemiParkinsonian mouse model. *Journal of Pharmacological Sciences*, *103*(3), 329–332. https://doi.org/10.1254/jphs.SCZ070058

Mercuri, N. B., & Bernardi, G. (2005). The 'magic' of L-dopa: Why is it the gold standard Parkinson's disease therapy? *Trends in Pharmacological Sciences*, *26*(7), 341–344. https://doi.org/10.1016/j.tips.2005.05.002

Millan, M. J. (2010). From the cell to the clinic: A comparative review of the partial D_2/D_3 receptor agonist and α2-adrenoceptor antagonist, piribedil, in the treatment of Parkinson's disease. *Pharmacology & Therapeutics*, *128*(2), 229–273. https://doi.org/10.1016/j.pharmthera.2010.06.002

Mizuno, Y., Hasegawa, K., Kondo, T., Kuno, S., & Yamamoto, M., Japanese Istradefylline Study Group (2010). Clinical efficacy of istradefylline (KW-6002) in Parkinson's disease: A randomized, controlled study. *Movement Disorders*, *25*(10), 1437–1443. https://doi.org/10.1002/mds.23107

Moreau, J. L., & Huber, G. (1999). Central adenosine A(2A) receptors: An overview. *Brain Research Reviews*, *31*(1), 65–82. https://doi.org/10.1016/s0165-0173(99)00059-4

Müller, C. E., & Ferré, S. (2007). Blocking striatal adenosine A2A receptors: A new strategy for basal ganglia disorders. *Recent Patents on CNS Drug Discovery*, *2*(1), 1–21. https://doi.org/10.2174/157488907779561772

Müller, T. (2015). The safety of istradefylline for the treatment of Parkinson's disease. *Expert Opinion on Drug Safety*, *14*(5), 769–775. https://doi.org/10.1517/14740338.2015.1014798

Olanow, C. W., & Schapira, A. H. (2013). Therapeutic prospects for Parkinson disease. *Annals of Neurology*, *74*(3), 337–347. https://doi.org/10.1002/ana.24011

Perez-Burgos, A., Prieto, G. A., Galarraga, E., & Bargas, J. (2010). Cav2.1 channels are modulated by muscarinic M1 receptors through phosphoinositide hydrolysis in neostriatal neurons. *Neuroscience*, *165*(2), 293–299. https://doi.org/10.1016/j.neuroscience.2009.10.056

Pérez-Garci, E., Bargas, J., & Galarraga, E. (2003). The role of Ca^{2+} channels in the repetitive firing of striatal projection neurons. *Neuroreport*, *14*(9), 1253–1256. https://doi.org/10.1097/00001756-200307010-00013.

Pérez-Ortega, J., Duhne, M., Lara-González, E., Plata, V., Gasca, D., Galarraga, E., Hernández-Cruz, A., & Bargas, J. (2016). Pathophysiological signatures of functional connectomics in parkinsonian and dyskinetic striatal microcircuits. *Neurobiology of Disease*, *91*, 347–361. https://doi.org/10.1016/j.nbd.2016.02.023.

Plata, V., Duhne, M., Pérez-Ortega, J., Hernández-Martinez, R., Rueda-Orozco, P., Galarraga, E., Drucker-Colín, R., & Bargas, J. (2013). Global actions of nicotine on the striatal microcircuit. *Frontiers in Systems Neuroscience*, *7*, 78. https://doi.org/10.3389/fnsys.2013.00078.

Prasad, K., de Vries, E. F. J., Elsinga, P. H., Dierckx, R. A. J. O., & van Waarde, A. (2021). Allosteric interactions between adenosine A2A and dopamine D2 receptors in heteromeric complexes: biochemical and pharmacological characteristics, and opportunities for PET imaging. *International Journal of Molecular Sciences*, *22*(4), 1719. https://doi.org/10.3390/ijms22041719.

Preti, D., Baraldi, P. G., Moorman, A. R., Borea, P. A., & Varani, K. (2015). History and perspectives of A2A adenosine receptor antagonists as potential therapeutic agents. *Medicinal Research Reviews*, *35*(4), 790–848. https://doi.org/10.1002/med.21344.

Prieto, G. A., Perez-Burgos, A., Fiordelisio, T., Salgado, H., Galarraga, E., Drucker-Colin, R., & Bargas, J. (2009). Dopamine D(2)-class receptor supersensitivity as reflected in Ca2 + current modulation in neostriatal neurons. *Neuroscience*, *164*(2), 345–350. https://doi.org/10.1016/j.neuroscience.2009.08.030.

Reddy, P., Martinez-Martin, P., Brown, R. G., Chaudhuri, K. R., Lin, J. P., Selway, R., Forgacs, I., Ashkan, K., & Samuel, M. (2014). Perceptions of symptoms and expectations of advanced therapy for Parkinson's disease: Preliminary report of a patient-reported outcome tool for advanced Parkinson's disease (PRO-APD). *Health and Quality of Life Outcomes*, *12*, 11. https://doi.org/10.1186/1477-7525-12-11

Rendón-Ochoa, E. A., Hernández-Flores, T., Avilés-Rosas, V. H., Cáceres-Chávez, V. A., Duhne, M., Laville, A., Tapia, D., Galarraga, E., & Bargas, J. (2018). Calcium currents in striatal fast-spiking interneurons: Dopaminergic modulation of Ca_V1 channels. *BMC Neuroscience*, *19*(1), 42. https://doi.org/10.1186/s12868-018-0441-0.

Richardson, P. J., Kase, H., & Jenner, P. G. (1997). Adenosine A2A receptor antagonists as new agents for the treatment of Parkinson's disease. *Trends in Pharmacological Sciences*, *18*(9), 338–344. https://doi.org/10.1016/s0165-6147(97)01096-1.

Salim, H., Ferré, S., Dalal, A., Peterfreund, R. A., Fuxe, K., Vincent, J. D., & Lledo, P. M. (2000). Activation of adenosine A1 and A2A receptors modulates dopamine D2 receptor-induced responses in stably transfected human neuroblastoma cells. *Journal of Neurochemistry*, *74*(1), 432–439. https://doi.org/10.1046/j.1471-4159.2000.0740432.x

Sheth, S., Brito, R., Mukherjea, D., Rybak, L. P., & Ramkumar, V. (2014). Adenosine receptors: Expression, function and regulation. *International Journal of Molecular Sciences*, *15*(2), 2024–2052. https://doi.org/10.3390/ijms15022024

Stacy, M. (2009). Medical treatment of Parkinson disease. *Neurologic Clinics*, *27*(3), 60. https://doi.org/10.1016/j.ncl.2009.04.009

Stromberg, I., Popoli, P., Müller, C. E., Ferré, S., & Fuxe, K. (2000). Electrophysiological and behavioural evidence for an antagonistic modulatory role of adenosine A2A receptors in dopamine D2 receptor regulation in the rat dopamine-denervated striatum. *European Journal of Neuroscience*, *12*(11), 4033–4037. https://doi.org/10.1046/j.1460-9568.2000.00288.x.

Tozzi, A., de Iure, A., Di Filippo, M., Tantucci, M., Costa, C., Borsini, F., Ghiglieri, V., Giampà, C., Fusco, F. R., Picconi, B., & Calabresi, P. (2011). The distinct role of medium spiny neurons and cholinergic interneurons in the D₂/A₂A receptor interaction in the striatum: Implications for Parkinson's disease. *Journal of Neuroscience*, *31*(5), 1850–1862. https://doi.org/10.1523/JNEUROSCI.4082-10.2011.

Tozzi, A., Tscherter, A., Belcastro, V., Tantucci, M., Costa, C., Picconi, B., Centonze, D., Calabresi, P., & Borsini, F. (2007). Interaction of A2A adenosine and D2 dopamine receptors modulates corticostriatal glutamatergic transmission. *Neuropharmacology*, *53*(6), 783–789. https://doi.org/10.1016/j.neuropharm.2007.08.006

Uchida, S., Soshiroda, K., Okita, E., Kawai-Uchida, M., Mori, A., Jenner, P., & Kanda, T. (2015). The adenosine A2A receptor antagonist, istradefylline enhances anti-parkinsonian activity induced by combined treatment with low doses of L-DOPA and dopamine agonists in MPTP-treated common marmosets. *European Journal of Pharmacology*, *766*, 25–30. https://doi.org/10.1016/j.ejphar.2015.09.028

Vilchis, C., Bargas, J., Pérez-Roselló, T., Salgado, H., & Galarraga, E. (2002). Somatostatin modulates Ca2 + currents in neostriatal neurons. *Neuroscience*, *109*(3), 555–567. https://doi.org/10.1016/s0306-4522(01)00503-6

Yabuuchi, K., Kuroiwa, M., Shuto, T., Sotogaku, N., Snyder, G. L., Higashi, H., Tanaka, M., Greengard, P., & Nishi, A. (2006). Role of adenosine A1 receptors in the modulation of dopamine D1 and adenosine A2A receptor signaling in the neostriatum. *Neuroscience*, *141*(1), 19–25. https://doi.org/10.1016/j.neuroscience.2006.04.047

Yang, S. N., Dasgupta, S., Lledo, P. M., Vincent, J. D., & Fuxe, K. (1995). Reduction of dopamine D2 receptor transduction by activation of adenosine A2a receptors in stably A2a/D2 (long-form) receptor co-transfected mouse fibroblast cell lines: Studies on intracellular calcium levels. *Neuroscience*, *68*(3), 729–736. https://doi.org/10.1016/0306-4522(95)00171-e6

Zhai, S., Tanimura, A., Graves, S. M., Shen, W., & Surmeier, D. J. (2018). Striatal synapses, circuits, and Parkinson's disease. *Current Opinion in Neurobiology*, *48*, 9–16. https://doi.org/10.1016/j.conb.2017.08.004

Abbreviations

SPN	Striatal projection neurons
iSPN	Indirect striatal projection neurons
dSPN	direct striatal projection neurons
PD	Parkinson's disease
Ca_V	High voltage gated calcium channels
D_2R	Dopamine D_2 receptor
$A_{2A}R$	Adenosine A_{2A} receptor
A2A-Cre	Tg(Adora2a-cre) KG139Gsat
6-OHDA	6-Hydroxydopamine
L-DOPA	L-3,4 dihidroxifenilalanine
MPTP	1-methyl-4-phenyl-l,2,3,6-tetrahydropyridine
iCa^{2+}	Calcium currents
NMDA	N-methyl-D- aspartate
NMDG	N-methyl-d glucamine
EGTA	Ethylene Glycol Tetraacetic Acid
HEPES	4-(2-Hydroxyethyl)piperazine-1-ethanesulfonic acid
TTX	Tetrodotoxin
CGS	CGS-21680: 4-[2-[[6-Amino-9-(*N*-ethyl-β-D-ribofuranuronamidosyl)-9*H*-purin-2-yl]amino]ethyl]benzenepropanoic acid hydrochloride